BARI-TH/400-2000
SISSA 107/2000/EP

Analytical description of quasivacuum oscillations of solar neutrinos

E. Lisi[a], A. Marrone[a], D. Montanino[b], A. Palazzo[a], and S.T. Petcov[c, d, *]

[a] *Dipartimento di Fisica and Sezione INFN di Bari, Via Amendola 173, I-70126 Bari, Italy*

[b] *Dipartimento di Scienza dei Materiali dell'Università di Lecce, Via Arnesano, I-73100 Lecce, Italy*

[c] *Scuola Internazionale Superiore di Studi Avanzati, Via Beirut 4, I-34014 Trieste, Italy*

[d] *Istituto Nazionale di Fisica Nucleare, Sezione di Trieste, Via Valerio 2, I-34127 Trieste, Italy*

Abstract

We propose a simple prescription to calculate the solar neutrino survival probability P_{ee} in the quasivacuum oscillation (QVO) regime. Such prescription is obtained by matching perturbative and exact analytical results, which effectively take into account the density distribution in the Sun as provided by the standard solar model. The resulting analytical recipe for the calculation of P_{ee} is shown to reach its highest accuracy ($|\Delta P_{ee}| \leq 2.6 \times 10^{-2}$ in the whole QVO range) when the familiar prescription of choosing the solar density scale parameter r_0 at the Mikheyev-Smirnov-Wolfenstein (MSW) resonance point is replaced by a new one, namely, when r_0 is chosen at the point of "maximal violation of adiabaticity" (MVA) along the neutrino trajectory in the Sun. The MVA prescription admits a smooth transition from the QVO regime to the MSW transition one. We discuss in detail the phase acquired by neutrinos in the Sun, and show that it might be of relevance for the studies of relatively short timescale variations of the fluxes of the solar ν lines in the future real-time solar neutrino experiments. Finally, we elucidate the role of matter effects in the convective zone of the Sun.

Typeset using REVTEX

*Also at: Institute of Nuclear Research and Nuclear Energy, Bulgarian Academy of Sciences, BG–1784, Sofia, Bulgaria.

I. INTRODUCTION

The solar neutrino problem [1], emerging as a deficit of the observed solar neutrino rates [2–8] with respect to standard solar model (SSM) predictions [1,9,10], can be explained through neutrino flavor oscillations [11], possibly affected by the presence of matter [12–14] (see [15,16] for reviews of oscillation solutions and [17,18] for recent analyses). The analysis of neutrino oscillations requires a detailed study of the evolution of the flavor states (ν_e, ν_x), ν_x being any linear combination of ν_μ and ν_τ, along the neutrino trajectory. In the simplest case, the active states (ν_e, ν_x) are assumed to be superpositions, through a mixing angle $\omega \in [0, \pi/2]$, of two vacuum mass eigenstates (ν_1, ν_2), characterized by a mass squared gap $\delta m^2 = m_2^2 - m_1^2 > 0$ (see, e.g., [19]).

The corresponding neutrino evolution equation in the flavor basis,

$$i \frac{d}{dx} \begin{pmatrix} \nu_e \\ \nu_x \end{pmatrix} = H \begin{pmatrix} \nu_e \\ \nu_x \end{pmatrix} \ , \tag{1}$$

involves then the following vacuum (v) and matter (m) terms in the Hamiltonian H,

$$H = H_v + H_m \tag{2}$$

$$= \frac{k}{2} \begin{pmatrix} -\cos 2\omega & \sin 2\omega \\ \sin 2\omega & \cos 2\omega \end{pmatrix} + \frac{1}{2} \begin{pmatrix} V & 0 \\ 0 & -V \end{pmatrix} \ , \tag{3}$$

with the usual definitions for the neutrino wavenumber in vacuum,

$$k = \delta m^2 / 2E \ , \tag{4}$$

and for the neutrino potential in matter,

$$V(x) = \sqrt{2}\, G_F\, N_e(x) \ , \tag{5}$$

$N_e(x)$ being the electron density at the point of neutrino trajectory in the Sun, located at radial distance x from the Sun center.[1] The $N_e(x)$ distribution is usually taken from SSM calculations [9,10].

The Hamiltonian H is diagonalized in the matter eigenstate basis (ν_{1m}, ν_{2m}) through the mixing angle in matter ω_m defined by

$$k_m \sin 2\omega_m = k \sin 2\omega \ , \tag{6}$$

$$k_m \cos 2\omega_m = k \cos 2\omega - V \ , \tag{7}$$

k_m being the neutrino wavenumber in matter,

$$k_m = k \sqrt{(\cos 2\omega - V/k)^2 + \sin^2 2\omega} \ . \tag{8}$$

---

[1] The solar neutrinos reaching the Earth move practically radially in the Sun. The effect of off-center trajectories is negligible for our results, see Appendix A.

In this work, we focus on approximate solutions of Eq. (1) for neutrino flavor transitions at relatively small values of $\delta m^2/E$ [20–24], characterizing the so-called quasivacuum oscillation (QVO) [25–28,17,18] regime[2],

$$\text{QVO} \;\leftrightarrow\; \delta m^2/E \lesssim 10^{-8}\ \text{eV}^2/\text{MeV}\ . \tag{9}$$

In order to define our goals more precisely, we recall that, both in the QVO regime and in the "Mikheyev-Smirnov-Wolfenstein" (MSW) [12,13] regime, which takes place at $\delta m^2 \gtrsim$ few $\times$ 10^{-8} eV^2/MeV, the solar ν_e survival probability at the Earth surface can be written as

$$P_{ee} = P_0 + P_1\ , \tag{10}$$

where P_0 is the average probability,

$$P_0 = \tfrac{1}{2} + \left(\tfrac{1}{2} - P_c\right) \cos 2\omega \cos 2\omega^0_m\ , \tag{11}$$

and P_1 is an oscillating term [21] (see also [22,30]),

$$P_1 = -\sqrt{P_c(1-P_c)}\cos 2\omega^0_m \sin 2\omega \cos(\Phi_{21} - \Phi_{22})\ . \tag{12}$$

The main ingredients of the above equations are: (i) The mixing angle in matter ω^0_m at the ν_e production point x_0, with $\omega^0_m \simeq \pi/2$ in the QVO regime; (ii) The level crossing (or jump) probability P_c of the transition from ν_{2m} at $x = x_0$ to ν_1 at the surface of the Sun ($x = R_\odot$); and the phase

$$\xi = \Phi_{21} - \Phi_{22}, \tag{13}$$

accumulated on the ν path from x_0 to the Earth surface, $x = L = 1$ A.U.,[3] where the phases Φ_{2i}, $i = 1, 2$, have a simple physical interpretation [21]: $\Phi_{2i} \equiv \Phi_{2i}(x_0, L) = \arg[A_{2i}(x_0, L)]$, A_{2i} being the probability amplitude of the transition $\nu_{2m}(x_0) \to \nu_i(L)$ between the initial matter-eigenstate $\nu_{2m}(x_0)$ and the final vacuum-mass eigenstate $\nu_i(L)$. The phase ξ can also be decomposed (see, e.g., Appendix A) as a sum of a "solar" phase ξ_s acquired on the path in the Sun ($x \in [x_0, R_\odot]$) and a "vacuum" phase ξ_v, acquired in vacuum ($x \in [R_\odot, L]$),

$$\xi = \xi_s + \xi_v \tag{14}$$

$$= \xi_s + k(L - R_\odot)\ . \tag{15}$$

---

[2]The lower part of the QVO range ($\delta m^2/E \lesssim 5 \times 10^{-10}$ eV^2/MeV) corresponds to the vacuum oscillation (VO) regime [29]. In this work, we do not explicitly distinguish the VO range, but simply treat it as part of the QVO range. Let us note that VO solutions of the solar ν problem are disfavored by the current data [7,17,18].

[3]In this work we consider only solar matter effects. Earth matter effects are not relevant in the QVO regime, while in the MSW regime in which effectively $P_1 \simeq 0$ [22], they can always be implemented through a modification of the expression for $P_{ee} \simeq P_0$, see the discussion in [27].

As a consequence of Eqs. (10)–(15), solving the neutrino evolution equation (1) basically reduces to calculating P_c and ξ_s. This task can be accomplished through numerical integration of Eq. (1) for $x \in [x_0, R_\odot]$, leading to "exact" solutions.[4] However, suitable approximations to the exact results are also useful, both to speed up the calculations and to clarify the inherent physics.

The starting point of such approximations is usually the analytical solution of Eq. (1) for the case of exponential density $N_e(x)$ in the Sun [20,21] (see also [31–34]). Deviations of the SSM density from the exponential profile can then be incorporated by an appropriate prescription for the choice of the scale height parameter

$$r_0(x) = -\left[\frac{d}{dx}\ln N_e(x)\right]^{-1} , \tag{16}$$

characterizing the realistic change of the electron density along the neutrino trajectory in the Sun. The exponential density analytical results are derived assuming that $r_0 = \text{const}$. A well-known and widely used prescription for precision calculations of the jump probability P_c in the MSW regime is to use the "running" scale height parameter $r_0(x)$ in Eq. (16), where for given $\delta m^2/E$ and for $\omega < \pi/4$, x is chosen to coincide with the MSW resonance point, $x = x_{\rm res}$ [35].

In the present work, we show how the analytical solution (Sec. II) and the "running resonance" prescription for r_0 (Sec. III) can be smoothly extended from the MSW range down to the QVO range, and we give a justification for our procedure. The extension is first achieved by matching the resonance prescription to a perturbative expression for P_c, in the limit of small k (Sec. III). A more satisfactory match is then reached (Sec. IV) by replacing the resonance prescription, $r_0 = r_0(x_{\rm res})$, which can be implemented only for $\omega < \pi/4$, with the "maximal violation of adiabaticity" (MVA) prescription, $r_0 = r_0(x_{\rm mva})$, where for given $\delta m^2/E$ and any given $\omega \in [0, \pi/2]$, $x_{\rm mva}$ is the point of the neutrino trajectory in the Sun at which adiabaticity is maximally violated (or, more precisely, the adiabaticity function has a minimum). We also show how the phase ξ_s can be easily and accurately calculated in the QVO range through perturbative expressions at $O(k^2)$, and discuss the conditions under which ξ_s might play a phenomenological role (Sec. V). In Sec. VI it is shown that the perturbative results essentially probe the low-density, convective zone of the Sun. Our final prescriptions for the calculation of P_c and ξ_s, summarized in Sec. VII, allow to calculate P_{ee} using Eqs. (10)–(12) with an accuracy $|\Delta P_{ee}| \lesssim 2.6 \times 10^{-2}$ in the whole QVO range. All technical details are confined in Appendixes A–E.

While this work was being completed, our attention was brought to the interesting work [36], where the QVO range is also investigated from a viewpoint that, although being generally different from ours, partially overlaps on the topic of adiabaticity violation. We have then inserted appropriate comments at the end of Sec. IV.

---

[4] In this work, high precision numerical results (which we will call "exact") for SSM density [9,10] are obtained through the computer codes developed in [27].

II. ANALYTICAL FORMS FOR P_c AND ξ_s

In this section we recall the analytical expressions for P_c and ξ_s, valid for an exponential density profile,

$$N_e(x) = N_e(0) \exp(-x/r_0) \ , \tag{17}$$

where $N_e(0)$ and r_0 are derived from a best fit to the SSM profile [9,10] (see Fig. 1 in [27]),

$$N_e(0) = 245 \ \mathrm{mol/cm}^3 \ , \tag{18}$$

$$r_0 = R_\odot/10.54 \ . \tag{19}$$

Assuming $N_e(x)$ as in Eq. (17), the neutrino evolution equation (1) can be solved exactly in terms of confluent hypergeometric functions [20,21,31,32,34]. The associated expression for P_c can be simplified [20] by making a zeroth order expansion of the confluent hypergeometric functions in the small parameter

$$|z| \equiv r_0 V(R_\odot) \simeq 0.165 \ , \tag{20}$$

and by using the asymptotic series expansion in the inverse powers of the large parameter

$$|z_0| \equiv r_0 V(x_0) \gtrsim 4.5 \times 10^2 \ , \tag{21}$$

where $x_0 \lesssim 0.25\, R_\odot$ (bulk of the neutrino production zone). Then one obtains the well-known "double exponential" form for P_c [20],

$$P_c = \frac{\exp(2\pi r_0 k \cos^2\omega) - 1}{\exp(2\pi r_0 k) - 1} \ . \tag{22}$$

Concerning the phase ξ_s, to zeroth order in $r_0 V(R_\odot)$ one gets a compact formula [21] (without using the asymptotic series expansion in $|z_0|^{-n}$),

$$\begin{aligned} \xi_s = & -2 \arg\Gamma(1-c) - \arg\Gamma(a-1) + \arg\Gamma(a-c) \\ & -r_0 k \ln[r_0 V(x_0)] + k(R_\odot - x_0) \ , \end{aligned} \tag{23}$$

where

$$a = 1 + i r_0 k \sin^2\omega \ , \tag{24}$$

$$c = 1 + i r_0 k \ . \tag{25}$$

Both Eqs. (22,23) are valid at any ω, including $\omega \geq \pi/4$.[5]

Let us note that the expression (10) for the probability P_{ee} with the average probability P_0 and the oscillating term P_1 given by Eqs. (11)–(15), (22) and (23) was shown [21,22] to assume the correct form in the VO, MSW transition and "large δm^2" (averaged oscillations) regimes.

---

[5]We remark that the restriction $\delta m^2 \cos 2\omega > 0$ made at the beginning of [20,21], which is equivalent to take $\omega < \pi/4$ for the usual choice $\delta m^2 > 0$, was basically functional to obtain $P_{ee} < 1/2$ in a certain region of the parameter space (as it was implied by the results of the Homestake experiment). However, such restriction does not play any role in the derivation of the Eqs. (22) and (23) in [20,21], although this was not emphasized at the time. This has also been recently noticed in [37].

III. THE MODIFIED RESONANCE PRESCRIPTION

In this section, we show how the resonance prescription for calculation of P_c (and P_{ee}), valid in the MSW regime and in the first octant of ω, can be modified to obtain accurate values for P_c also for $k \to 0$ and for $\omega \gtrsim \pi/4$.

The resonance prescription in the MSW range is based on the following approximations: (i) oscillations are assumed (and where shown in [22]) to be averaged out, so that effectively $P_1 \simeq 0$ and ξ_s becomes irrelevant[6]; (ii) P_c is taken from Eq. (22), but with a variable scale height parameter $r_0 = r_0(x)$ [Eq. (16)], with x "running" with the resonance (RES) point $x = x_{\rm res}$ [35],

$$r_0 = r_0(x_{\rm res}) \ , \tag{26}$$

where $x_{\rm res}$ is defined by the resonance condition [13,14]

$$\cos 2\omega_m(x_{\rm res}) = 0 \ , \tag{27}$$

when applicable. In the absence of resonance crossing, it was customary to take $P_c = 0$ in the MSW regime (see, e.g., [38]). In particular, in the MSW analysis of [39], $P_c = 0$ was taken in the second octant of ω, where $\cos 2\omega_m < 0$ and Eq. (27) is never satisfied.

The indicated resonance prescription for the calculation of P_c is known to work very well over at least three decades in $\delta m^2/E$ ($\sim 10^{-7}$–10^{-4} eV^2/MeV) [35], with a typical accuracy of a few $\times 10^{-2}$ in P_{ee}. However, in the lowest MSW decade ($\delta m^2/E \sim 10^{-8}$–$10^{-7}$ eV^2/MeV), such prescription is not very accurate both in the first octant [35] (where it tends to underestimate the effective value of r_0) and in the second octant [25] (where P_c is small but not exactly zero). It was found numerically in [35] that, for small k, a relatively small and constant value of r_0 ($\simeq R_\odot/15.4$) provided a better approximation to P_0 in the first octant[7]; this observation has been also discussed and extended to the second octant in [25] (where $r_0 \simeq R_\odot/18.4$ is used for $k \to 0$). Here we derive (and improve) such prescriptions by means of perturbation theory.

The key result is worked out in Appendix B, where we find a perturbative solution of the neutrino evolution equation (1), in the limit of small values k, by treating the vacuum term H_v as a perturbation of the dominant matter term H_m in the Hamiltonian [Eq. (3)]. The $O(k)$ solution[8] can be expressed in terms of the following dimensionless integral,

$$I_\eta = \int_0^1 d\rho \, \exp\left(i \int_\rho^1 d\rho' V(\rho') R_\odot \right) \ , \tag{28}$$

---

[6]The same conclusion is valid for all other oscillating terms (and their phases) in P_{ee} [21,22].

[7]The numerical results for P_0 were obtained in [35] by using the density $N_e(x)$ provided by the Bahcall-Ulrich 1988 standard solar model [40].

[8]The perturbative expansion can be expressed in terms of dimensionless parameters such as $kR_\odot$ or kr_0. However, for simplicity, we use the notation $O(k^n)$, $k \to 0$ etc., instead of $O(k^n R_\odot^n)$, $kR_\odot \to 0$, etc.

where $\rho = x/R_\odot$, and $V(x)$ is given by Eq. (5). In particular, the effective value of r_0 (in the limit of small k) is given by $2\pi^{-1} R_\odot \, \mathrm{Im}(I_\eta)$, namely,

$$\lim_{k\to 0} r_0 = \frac{2}{\pi} R_\odot \int_0^1 d\rho \, \sin\left(\int_\rho^1 d\rho' \sqrt{2}\, G_F \, N_e(\rho') \, R_\odot \right) \; , \tag{29}$$

independently of ω (i.e., both in the first and in the second octant).

The above perturbative results show that the asymptotic ($k \to 0$) effective value for r_0 depends upon a well-defined integral over the density profile $N_e(x)$. Using the SSM profile for $N_e(x)$ [9,10], we find that

$$\lim_{k\to 0} r_0 = R_\odot/18.9 \; . \tag{30}$$

The same value is obtained through exact numerical calculations.

The appearance of integrals over the whole density profile indicates that, for small k, the behavior of P_c becomes nonlocal, as was also recently noticed in [36]. We further elaborate upon the issue of nonlocality in Sec. VI, where we show that the $O(k)$ perturbative results are actually dominated by matter effects in the convective zone of the Sun ($x/R_\odot \gtrsim 0.7$), where the function $N_e(x)$ resembles a power law rather than an exponential.

In order to match the usual resonance prescription [$r_0 = r_0(x_{\rm res})$] with the value $r_0 = R_\odot/18.9$ in the regime of small k, we observe that, for the SSM density distribution [9,10] it is $r_0(x) = R_\odot/18.9$ at $x = 0.904\, R_\odot$. Thus, we are naturally led to the following "modified resonance prescription,"

$$r_0 = \begin{cases} r_0(x_{\rm res}) & \text{if } x_{\rm res} \leq 0.904\, R_\odot \; , \\ R_\odot/18.9 & \text{otherwise} \; , \end{cases} \tag{31}$$

where "otherwise" includes cases with $\omega \geq \pi/4$, for which $x_{\rm res}$ is not defined. Such a simple recipe provides a description of P_c which is continuous in the mass-mixing parameters, and is reasonably accurate both in the QVO range ($\delta m^2/E \lesssim 10^{-8}$ eV^2/MeV) and in the lowest MSW decade ($\delta m^2/E \simeq$ few $\times\, 10^{-8}$–10^{-7} eV^2/MeV).

Figure 1 shows isolines of P_c in the bilogarithmic plane charted by the variables[9] $\delta m^2/E \in [10^{-10}, 10^{-7}]$ eV^2/MeV and $\tan^2\omega \in [10^{-3}, 10]$.[10] The solid lines refer to the exact numerical calculation of P_c, while the dotted lines are obtained through the analytical formula for P_c [Eq. (22)], supplemented with the modified resonance prescription [Eq. (31)]. Also shown are, in the first octant, isolines of resonance radius for $x_{\rm res}/R_\odot = 0.6$, 0.7, 0.8, and 0.904. The maximum difference between the exact (numerical) results and those obtained using the analytic expression for P_c, Eq. (22), amounts to $|\Delta P_c| \simeq 7.5 \times 10^{-2}$, and is typically much smaller. Since P_c is not a directly measurable quantity, we propagate the results of

---

[9]In all the figures of this work, we extend the $\delta m^2/E$ interval somewhat beyond the QVO range, in order to display the smooth transition to the MSW range.

[10]The variable $\tan^2\omega$ was introduced in [39] to chart both octants of the solar ν mixing angle ω in logarithmic scale.

Fig. 1 to probability amplitudes observable at the Earth, namely, to the average probability P_0 [Eq. (11)] and to the prefactor of the oscillating term P_1 [Eq. (12)].[11]

Figure 2 shows isolines of P_0 for SSM density, derived numerically (solid lines) and by using the analytic expression for P_0 and the modified resonance prescription (dotted lines). The maximum difference is $|\Delta P_0| \simeq 3.4 \times 10^{-2}$. Figure 3 shows, analogously, isolines of $P_1/\cos\xi$. The difference amounts to $|\Delta(P_1/\cos\xi)| \lesssim 12.5 \times 10^{-2}$.

From Figs. 1–3, the modified resonance prescription for r_0 [Eq. (31)] emerges as a reasonable and remarkably simple approximation to the exact results for P_c, valid in both the MSW and the QVO regimes. However, it does not reproduce the exact behavior of P_c with the requisite high precision of few % for $\delta m^2/E \sim O(10^{-8})$ eV^2/MeV and $\tan^2\omega \sim O(1)$. This difference can be understood and removed, to a large extent, through the improved prescription discussed in the next Section.

IV. THE PRESCRIPTION OF MAXIMUM VIOLATION OF ADIABATICITY

In this section we generalize and improve Eq. (31), by replacing the point of resonance ($x_{\rm res}$) with the point where adiabaticity is maximally violated ($x_{\rm mva}$), more precisely, where the adiabaticity function has its absolute minimum on the neutrino trajectory.

Let us recall that the validity of the resonance prescription $r_0 = r_0(x_{\rm res})$ is based on the fact that $P_c \neq 0$ in a relatively shorth part of the ν trajectory, where the propagation is locally nonadiabatic. The resonance condition, however, can be fulfilled only in the first octant of ω. The most general condition for nonadiabaticy, as introduced already in the early papers [13,35,41,42] on the subject, has instead no particular restriction in ω [43]. Such alternative condition can be expressed, in the basis (ν_{1m}, ν_{2m}) relevant for the calculation of P_c, in terms of the ratio between the diagonal term ($\pm k_m/2$) and the off-diagonal term ($\pm i d\omega_m/dx$) in the (traceless) Hamiltonian. More specifically, a transition is nonadiabatic if the ratio

$$\gamma(x) \equiv \frac{k_m(x)}{|2d\omega_m(x)/dx|} = \frac{k^2 \sin^2 2\omega}{|dV(x)/dx|}\left(1 + \frac{(\cos 2\omega - V(x)/k)^2}{\sin^2 2\omega}\right)^{3/2} , \qquad (32)$$

satisfies the inequality $\gamma(x) \lesssim 1$ at least in one point of the neutrino trajectory in the Sun. If $\gamma(x)$ is large along the whole trajectory, $\gamma(x) \gg 1$, the transition is adiabatic. The minimal value of $\gamma(x)$ identifies the point of "maximum violation of adiabaticity," $x_{\rm mva}$,

$$\gamma(x_{\rm mva}) \equiv \min\gamma(x) \ . \qquad (33)$$

We show in Appendix B, that, along the solar ν trajectory, the MVA point is uniquely defined, for any ω in both octants. In particular, such point can be unambiguously characterized through the condition[12]

---

[11] The phase ξ is separately studied in Sec V.

[12] A handy approximation to the MVA condition, which by-passes the calculation of derivatives with a modest price in accuracy, is discussed at the end of Appendix B.

$$\frac{d^2 \cos 2\omega_m}{dx^2} = 0 \quad \text{at } x = x_{\rm mva} \ . \tag{34}$$

In the first octant, in general, $x_{\rm mva}$ differs from $x_{\rm res}$, although one can have $x_{\rm mva} \simeq x_{\rm res}$ in some limiting cases (see Appendix B for a more general discussion). For instance, as Eq. (32) indicates, the two points practically coincide, $x_{\rm mva} \simeq x_{\rm res}$, in the case of nonadiabtic transitions at small mixing angles ($\sin^2 2\omega \ll 1$). Indeed, let us consider for illustration the simplified exponential case of $r_0 = {\rm const}$. In this ("exp") case it is easy to find from Eq. (32) that:

$$x^{\rm exp}_{\rm res} - x^{\rm exp}_{\rm mva} = r_0 \ln \frac{1}{4} \left(1 + \sqrt{1 + 8(1 + \tan^2 2\omega)} \right) \ . \tag{35}$$

Obviously, at small mixing angles ($\tan^2 2\omega \ll 1$) we have $x_{\rm mva} \simeq x_{\rm res}$. However, this is no longer true for the nonadiabatic transitions at large mixing angles in the QVO regime we are interested in. In the latter case, as it follows from Eq. (35), $x_{\rm mva} < x_{\rm res}$.

We discuss in Appendix B the more realistic case of SSM density. As far as the calculation of P_c is concerned, it turns out that $x_{\rm mva} \to x_{\rm res}$ in the limits of small ω (or of large k). Therefore, the MVA condition smoothly extends the more familiar resonance condition in both directions of large mixing and of small k, which are relevant to pass from the MSW to the QVO regime. The inequality $x_{\rm mva} < x_{\rm res}$, derived for exponential density, persists in the QVO range for the realistic case of SSM density, implying that

$$r_0(x_{\rm mva}) > r_0(x_{\rm res}) \ , \tag{36}$$

with $r_0(x)$ defined as in Eq. (16). As a conseqence, a difference arises in the value of P_c if $x_{\rm res}$ is replaced by $x_{\rm mva}$ in the prescription for calculating r_0.

Explicitly, our MVA prescription reads

$$r_0 = \begin{cases} r_0(x_{\rm mva}) & \text{if } x_{\rm mva} \leq 0.904\, R_\odot \ , \\ R_\odot/18.9 & \text{otherwise} \ . \end{cases} \tag{37}$$

Figure 4 shows curves of iso-r_0 obtained through Eq. (37). The value of r_0 presents weak variations (within a factor of two) in the whole mass-mixing plane and, by construction, smoothly reaches the plateau $r_0 = R_\odot/18.9$ for $\delta m^2 \lesssim$ few $\times\, 10^{-9}$ eV^2/MeV.

Figures 5, 6, and 7 are analogous to Figs 1, 2 and 3, respectively, modulo the replacement of the resonance condition [Eq. (31)] with the MVA condition [Eq. (37)]. The MVA prescription clearly improves the calculation of P_c, P_0, and $P_1/\cos\xi$, with an accuracy better than a few percent in the whole plane plotted: $|\Delta P_c| \lesssim 3.7 \times 10^{-2}$, $|\Delta P_0| \lesssim 2.5 \times 10^{-2}$, $|\Delta(P_1/\cos\xi)| \lesssim 3.3 \times 10^{-2}$.

We conclude that the analytical formula for P_c [Eq. (22)], valid for an exponential density, can be applied with good accuracy to the case of SSM density, provided that the scale height parameter r_0 is chosen according to the MVA prescription, Eq. (37).

A final remark is in order. We agree with the author of [36] about the fact that, in order to understand better the behavior of P_c in the QVO regime, the concept of adiabaticity violation *on the whole neutrino trajectory* is to be preferred to the concept of adiabaticity violation *at the resonance point*. However, we do not share his pessimism about the possibility of

using the running value $r_0(x_{\rm mva})$ for accurate calculations of P_c: indeed, Figs. 5-7 just demonstrate this possibility. Such pessimism seems to originate from the observation that, as k decreases, P_c starts to get nonlocal contributions from points rather far from $x_{\rm mva}$ [36]. In our formalism, this behavior shows up in the $k \to 0$ limit [Eq. (30)], where, as mentioned in the previous Section, the effective value of r_0 gets contributions from an extended portion of the density profile [see also Sec. VI and Appendix C for further discussions]. Our prescription (37), however, effectively takes this fact into account, by matching the "local" behavior of r_0 for large k [$r_0 = r_0(x_{\rm mva})$] with the "nonlocal" behavior of r_0 at small k [$r_0 = R_\odot/18.9$]. In conclusion, the MVA prescription, appropriately modified [Eq. (37)] to match the $k \to 0$ limit, allows a description of P_c which is very accurate in the whole QVO range, and which smoothly matches the familiar resonance prescription up in the MSW range.

V. THE PHASE ξ_s ACQUIRED IN THE SUN

In this Section, we discuss the last piece for the calculation of P_{ee}, namely, the solar phase ξ_s. As we will see, this phase can significantly affect the quasivacuum oscillations of almost "monochromatic" solar neutrinos (such as those associated to the ^{7}Be and *pep* spectra). Indeed, there might be favorable conditions in which the phase ξ_s (often negligible in current practical calculations) could lead to observable effects and should thus be taken into account.

First, let us observe that, in the QVO range, the size of the solar phase ξ_s is of $O(kR_\odot)$, as indicated by Eq. (23) for exponential density [21], and also confirmed through numerical calculations for SSM density [27]. Figure 9 shows, in particular, exact results for the ratio $\xi_s/kR_\odot$, as a function of $\delta m^2/E$, using the SSM density. It appears that, neglecting ξ_s with respect to the vacuum phase ξ_v, is almost comparable to neglect $R_\odot$ as compared with L. Remarkably, there are cases in which corrections of $O(R_\odot/L)$ are nonnegligible, e.g., in the study of time variations of P_{ee} over short time scales [22–24,44], induced by the Earth orbit eccentricity ($\varepsilon = 0.0167$). In fact, the fractional monthly variation of $L(t)$ from aphelion to perihelion is $2\varepsilon L/6 = 1.2\, R_\odot$. Real-time experiments aiming to detect time variations of the ν flux in monthly bins might thus test terms of $O(R_\odot/L) \sim O(\xi_s/\xi_v)$, as also emphasized at the end of Sec. VI in the work [27].

Secondly, let us recall that the oscillating term $\cos\xi$ gets averaged to zero when the total phase ξ is very large [22]. The approximation $\langle\cos\xi\rangle \simeq 0$ holds in the MSW regime, but it becomes increasingly inaccurate (and is eventually not applicable) as k decreases down to the QVO regime. In order to understand when ξ starts to be observable (at least in principle) one can consider an optimistic situation, namely, an ideal measurement of P_{ee} with a real-time detector having perfect energy resolution, and monitoring the flux from narrowest solar ν spectra (the Be and *pep* neutrino lines). In this case, the most important—and basically unavoidable—source of smearing is the energy integration [22,45,46,44,47] over the ν lineshape.[13] It has been shown in [27] (see also [22,24]) that such integrations effectively suppresses the oscillating term P_1 at the Earth through a damping factor D,

[13]Smearing over the ν production zone is irrelevant in the QVO regime [27], see also Appendix A.

calculable in terms of the ν lineshape. Figure 8 shows the factor D for the *pep* line and the for two Be lines, characterized by average energies $\langle E \rangle = 1442$, 863.1, and 385.5 keV, respectively. The Be and *pep* lineshapes [having $O(1)$ keV widths] have been taken from [48] and [44], respectively. Figure 8 proves that ξ is observable, at least in principle, in the whole QV range $\delta m^2/E \lesssim 10^{-8}$ eV^2/MeV, as far as the narrowest Be line is considered. Of course, the observability of ξ becomes more critical (or even impossible) by increasing the initial energy spread (e.g., for continuous ν spectra) or by performing measurements (like in current experiments) with additional and substantial detection smearing in the energy or time domain [22].

With the above caveats in mind, we set out to describe accurately ξ_s in the whole QVO range. This task is accomplished in Appendixes D and E where, by means of the same perturbative method applied earlier to P_c, we obtain the $O(k)$ and $O(k^2)$ expressions for ξ_s, respectively. The final perturbative result is

$$\xi_s \simeq 0.130\,(k\,R_\odot) + 1.67 \times 10^{-3} (k\,R_\odot)^2 \cos 2\omega + O(k^3)\ , \tag{38}$$

which is in excellent agreement with the exact result for ξ_s shown in Fig. 9, in the whole QVO range.

The $O(k)$ coefficient in Eq. (38) is just the real part of the integral I_η in Eq. (28) (see Appendix D) and is already sufficient for an accurate description of ξ_s in the QVO range. Remarkably, the right magnitude of this coefficient can also be obtained from the analytical expression (23), which would give $\xi_s \simeq 0.116\,kR_\odot$ (see Appendix D). We also keep the small $O(k^2)$ term in Eq. (38), because it neatly shows that ξ_s starts to become ω-dependent for increasing values of $\delta m^2/E$, consistently with the exact numerical results of Fig. 9.

Figure 10 shows the error one makes on the phase ξ_s, by using increasingly better approximations, for two representative values of $\tan^2\omega$. The error is given as the absolute difference between approximate and exact results for ξ_s, in units of a period (2π). The lowest possible approximation is simply to neglect $R_\odot$ with respect to L, so that $\xi = kL$ and $\xi_s = kR_\odot$, namely, neutrino oscillations are effectively started at the Sun center ("empty Sun"). A better approximation is to start oscillations at the sun edge, $\xi = k(L - R_\odot)$ and $\xi_s = 0$, by assuming that the high sun density damps oscillations up to the surface [12,49] ("superdense Sun"). Such two approximations (and especially the first) are widely used in phenomenological analyses. Figure 10 shows, however, that they can produce a considerable phase shift (even larger than a full period for the case of "empty" Sun) in the upper QVO range. The fact that the SSM density is neither $N_e = 0$ nor $N_e = \infty$ is correctly taken into account through the $O(k)$ term in Eq. (38), and even more accurately through the full $O(k^2)$ expression for ξ_s in Eq. (38), as evident from Fig. 10.

The errors estimated in Fig. 10 show that different approximations for ξ_s can affect calculations for future experiments. In particular, the use of the familiar "empty Sun" or "superdense Sun" approximations can possibly generate fake phase shifts in time variation analyses for real-time detectors sensitive to neutrino lines, such as Borexino [50] or KamLAND [51]. According to the estimates in [52], such two experiments might be sensitive to monthly-binned seasonal variations for $\delta m^2 \lesssim 5 \times 10^{-9}$. Figure 10 shows that, in the upper part of such sensitivity range, the empty Sun approximation gives ξ_s (and thus ξ) totally out of phase, as compared with exact results. Analogously, the superdense Sun approximation

induces a phase shift that, although smaller than in the previous case, can still be as large as $\pi/2$ ($\Delta\xi_s \lesssim 0.2 \times 2\pi \sim \pi/2$) in the quoted sensitivity range, and can thus produce a big difference [$\Delta \cos\xi \simeq O(1)$] in the calculation of P_1.

It is an unfortunate circumstance, however, that the dominant term in ξ_s is proportional to k. This fact implies that, neglecting $\xi_s \simeq 0.130 R_\odot/L$ in the total phase $\xi = \xi_v + \xi_s$, is basically equivalent to introduce a small bias of the kind $\delta m^2 \to \delta m^2 \times (1 + 0.130\, R_\odot/L) = \delta m^2 \times (1 + 6 \times 10^{-4})$. On one hand, such bias is sufficient to produce a substantial difference in $\cos\xi$ when $\delta m^2/E$ approaches 10^{-8} eV^2/MeV, and is thus observable in principle. On the other hand, δm^2 is not known a priori, but must be derived from the experiments themselves, and it will be hardly known with a precision of $O(\text{few} \times 10^{-4})$ for some time. Therefore, although ξ_s may produce a big effect at *fixed* values of δm^2, it might be practically obscured by uncertainties in the *fitted* value of δm^2.

In conclusion, we have found a simple and accurate expression for the solar phase ξ_s, to be used in the calculation of the total phase $\xi = \xi_s + k(L - R_\odot)$. The solar phase ξ_s produces effects of $O(R_\odot/L)$, which can be nonnegligible in high-statistics, real-time experiments sensitive to short-time variations associated to neutrino lines, such as Borexino and KamLAND, as was also emphasized in [22,23] and more recently in [27]. In such context, we recommend the use of Eq. (38) for precise calculations of P_{ee} at fixed value of δm^2, although the observability of ξ_s certainly represents a formidable challenge.

VI. PROBING THE CONVECTIVE ZONE OF THE SUN

In this section we elaborate upon the $O(k)$ perturbative results discussed previously for P_c and ξ_s (and detailed in Appendix C and D). In particular, we show that they are related to the density in the convective zone of the Sun, corresponding to $\rho = x/R_\odot \gtrsim 0.7$.

The $O(k)$ results crucially depend upon the quantity I_η, which is defined in Eq. (28) as an integral over an oscillating function, having the density $N_e(x)$ as inner argument. Numerical evaluation of such integral for SSM density gives $I_\eta = (13.03 + i\, 8.32) \times 10^{-2}$ (see Appendix C). It turns out that the largest contribution to I_η comes from the outer regions of the Sun, where the integrand oscillates slowly, while in the inner regions the integrand oscillates rapidly, with vanishing net contribution to the real and imaginary parts of I_η. Numerical inspection shows that the value of I_η is dominated by the $\rho \gtrsim 0.7$ range, which happens to correspond to the convective zone of the Sun [1]. Therefore, it is sufficient to consider such zone to estimate I_η.

In the convective zone, the density profile $N_e(x)$ is better described by a power law rather than by an exponential function (see, e.g., [53]). A good approximation to the SSM density for $\rho \gtrsim 0.7$ is:

$$N_e(\rho) \simeq N_p (1 - \rho)^{p-1} \ , \tag{39}$$

with $p \simeq 2.8$ and $N_p \simeq 1.4$ mol/cm^3. By adopting such expression for the density, and using the position $z = 1 - \rho$, we get the following expression for I_η,

$$I_\eta = \int_0^1 dz\, \exp(iqz^p) \ , \tag{40}$$

where $q = V_p R_\odot/p \simeq 135$ and $V_p = \sqrt{2} G_F N_p$. Once again, we note that the above integrand gives a very small contribution outside the convective zone ($z \gtrsim 0.3$), since the exponent becomes large. Therefore, the upper limit can be shifted from 1 to ∞ without appreciable numerical changes, and with the advantage that the result can be cast in a compact analytical form, reproducing the exact SSM numerical result with good accuracy:

$$I_\eta \simeq \int_0^\infty dz \, \exp(iqz^p) \tag{41}$$

$$= q^{-1/p} \Gamma(1 + p^{-1}) e^{i\frac{\pi}{2p}} \tag{42}$$

$$\simeq (13 + i\, 8.2) \times 10^{-2} \ . \tag{43}$$

Using the above equation and the results of Appendixes C and D, the small-k limit for r_0 and ξ_s can be explicited as

$$\frac{r_0}{R_\odot} \simeq \frac{2}{\pi} \, q^{-1/p} \, \Gamma(1 + p^{-1}) \, \sin(\pi/2p) \ , \tag{44}$$

$$\frac{\xi_s}{k R_\odot} \simeq q^{-1/p} \, \Gamma(1 + p^{-1}) \, \cos(\pi/2p) \ . \tag{45}$$

Such results show that the effective values of r_0 and of ξ_s at small k are connected to the parameters (p, q) describing the power-law dependence of $N_e(x)$ in the convective zone of the Sun [Eq. (39)]. Therefore, while for relatively large k neutrino oscillations in matter probe the inner "exponential bulk" of the solar density profile, for small k they mainly probe the outer, "power-law" zone of convection.

Finally, let us notice that, in the range $0.7 \lesssim \rho \lesssim 0.9$, where the "running" MVA prescription $r_0 = r_0(x_{\rm mva})$ is applicable, the power law in Eq. (39) leads to $r_0(x)/R_\odot = (1 - \rho)/(p - 1)$, so that $r_0(x)/R_\odot \simeq 1/18.9$ at the matching point $\rho \simeq 0.904$, consistently with the prescription in Eq. (37).

VII. SUMMARY OF RECIPES FOR CALCULATION OF P_{ee} IN THE QVO REGIME

We summarize our best recipe for calculation of P_{ee} as follows. In the QVO regime, for any given value of the mixing angle ω and of the neutrino wavenumber $k = \delta m^2/2E$, the ν_e survival probability reads

$$P_{ee} = P_c \cos^2\omega + (1 - P_c) \sin^2\omega + \sin 2\omega \sqrt{P_c(1 - P_c)} \cos\xi \ ,$$

where

$$\xi = \xi_s + k(L - R_\odot) \ .$$

The value of P_c can be evaluated with high precision by using the analytical form

$$P_c = \frac{\exp(2\pi r_0 k \cos^2\omega) - 1}{\exp(2\pi r_0 k) - 1} \ ,$$

provided that the density scale parameter r_0 is calculated as

$$r_0 = \begin{cases} r_0(x_{\rm mva}) & \text{if } x_{\rm mva} \leq 0.904\, R_\odot \ , \\ R_\odot/18.9 & \text{otherwise} \ , \end{cases}$$

where $x_{\rm mva}$ is the point where adiabaticity is maximally violated along the neutrino trajectory in the Sun (see Appendix B). Such expression for P_c smoothly joins the more familiar resonance prescription when passing from the QVO to the MSW regime.

The value of the Sun phase ξ_s can be calculated with high precision by using the $O(k^2)$ perturbative result, valid for $\delta m^2/E \lesssim 10^{-8}$ eV^2/MeV,

$$\xi_s \simeq 0.130\,(k\,R_\odot) + 1.67 \times 10^{-3} (k\,R_\odot)^2 \cos 2\omega \ .$$

We have shown that such phase can play a role in precise calculations of P_{ee} in the QVO range. It is not necessary to extend the calculation of ξ_s in the MSW range, where effectively $\langle \cos\xi \simeq 0 \rangle$, and ξ_s is not observable even in principle. Notice that the neutrino production point x_0 does not appear in the calculation of both P_c and ξ_s in the QVO range.

Finally, we have checked that the above recipe allows the calculation of P_{ee} with an accuracy $|\Delta P_{ee}| \lesssim 2.6 \times 10^{-2}$ (and often much better than a percent) in both octants of ω for the whole QVO range ($\delta m^2 \lesssim 10^{-8}$ eV^2/MeV). Figure 11 shows, as an example, a graphical comparison with the exact results for P_{ee} at the exit from the Sun ($x = R_\odot$).[14] It appears at glance that our recipe represents an accurate substitute to exact numerical calculations of P_{ee}, in the whole QVO range $\delta m^2/E \lesssim 10^{-8}$ eV^2/MeV.

VIII. CONCLUSIONS

We have worked out a simple and accurate prescription to calculate the solar neutrino survival probability P_{ee} in the quasivacuum oscillation regime. Such prescription adapts the known analytical solution for the exponential case to the true density case, as well as to the perturbative solution of neutrino evolution equations in the limit of small $\delta m^2/E$. The accuracy of the prescription is significantly improved (up to 2.6×10^{-2} in P_{ee} in the whole QVO range) by replacing the familiar prescription of choosing the scale height parameter r_0 at the MSW resonance point by a new one: r_0 is chosen at the point of maximal violation of adiabaticity (MVA) along the neutrino trajectory in the Sun. Such generalization preserves a smooth transition of our prescription from the QVO to the MSW oscillation regime, where the two prescriptions practically coincide. We show that at sufficiently small $k = \delta m^2/2E$ in the QVO regime, the effective value of r_0 is determined by an integral over the electron density distribution in the Sun, $N_e(x)$:

$$\lim_{k\to 0} r_0 = \frac{2}{\pi} R_\odot \int_0^1 d\rho \, \sin\left(\int_\rho^1 d\rho' \, \sqrt{2}\, G_F \, N_e(\rho')\, R_\odot \right) \ ,$$

[14] The function P_{ee} at the Earth ($x = L$) can not be usefully plotted in the range of Fig. 11, due to its rapidly oscillating behavior.

where $\rho = x/R_\odot$. The main contribution in the above integral is shown to come from the region corresponding to the convective zone of the Sun, $x \gtrsim 0.7 R_\odot$. Thus, if quasivacuum oscillations take place, solar neutrino experiments might provide information about the density distribution in the convective zone of the Sun. We also discuss in detail the phase acquired by neutrinos in the Sun, whose observability, although possible in principle, poses a formidable challenge for future experiments aiming to observe short timescale variations of fluxes from solar ν lines.

ACKNOWLEDGMENTS

A.M. acknowledges kind hospitality at SISSA during the initial stage of this work. S.T.P. would like to acknowledge the hospitality of the Aspen Center for Physics where part of this work was done. The work of E.L., A.M., and A.P. was supported in part by the Italian MURST under the program "Fisica Astroparticellare." The work of S.T.P. was supported in part by the EEC grant ERBFMRXCT960090 and by the Italian MURST under the program "Fisica Teorica delle Interazioni Fondamentali."

APPENDIX A: GENERAL FORM OF P_{ee} AND ITS QV LIMIT

In this Appendix we recall the derivation of the basic equations for P_{ee} given in the Introduction, together with further details relevant for Appendixes B–E.

Given an initial solar ν_e state $\Psi_e = (1,0)^T$ (T being the transpose), its final survival amplitude A_{ee} at the detector can be factorized as

$$A_{ee}(x_0, L) = \Psi_e^T \, U_\omega \, U_v \, U_m \, U_{\omega_m^0}^T \, \Psi_e \tag{A1}$$

$$= \Psi_e^T \begin{pmatrix} \cos\omega & \sin\omega \\ -\sin\omega & \cos\omega \end{pmatrix} \begin{pmatrix} e^{i\xi_v/2} & 0 \\ 0 & e^{-i\xi_v/2} \end{pmatrix} \times \begin{pmatrix} \sqrt{1-P_c}\, e^{-i\alpha} & -\sqrt{P_c}\, e^{-i\beta} \\ \sqrt{P_c}\, e^{i\beta} & \sqrt{1-P_c}\, e^{i\alpha} \end{pmatrix} \begin{pmatrix} \cos\omega_m^0 & -\sin\omega_m^0 \\ \sin\omega_m^0 & \cos\omega_m^0 \end{pmatrix} \Psi_e \ , \tag{A2}$$

where the U matrices act as follows (from right to left): (i) $U_{\omega_m^0}^T$ rotates (at $x = x_0$) the initial state N_e into the matter mass basis; (ii) U_m is a generic $SU(2)$ parametrization for the evolution of the matter mass eigenstates (ν_{1m}, ν_{2m}) from the origin ($x = x_0$) up to the exit from the Sun ($x = R_\odot$) where $\nu_{im} = \nu_i$, in terms of the so-called crossing probability $P_c = P(\nu_{2m} \to \nu_1)$ and of two generic phases α and β; (*iii*) U_v evolves the mass eigenstates in vacuum along one astronomical distance L, with ξ_v defined in Eq. (15); and (*iv*) U_ω finally rotates the mass basis back to the flavor basis at the detection point ($x = L$).[15]

[15]During nighttime, one should insert a fifth matrix to take into account the evolution within the Earth, which we do not consider in this work (focussed on solar matter effects in the QVO range). Earth matter effects can always be added afterwards as a calculable modification to P_0, since they turn out to be nonnegligible only in the MSW regime, when oscillations are averaged out and $P_1 \simeq 0$, see [27] and references therein.

After some algebra, the resulting ν_e survival probability can be expressed as the sum of an "average term" P_0 plus four "oscillating terms" [21,30],

$$P_{ee} = |A_{ee}(x_0, L)|^2 = \sum_{n=0}^{4} P_n \ , \tag{A3}$$

where

$$P_0 = \frac{1}{2} + \left(\frac{1}{2} - P_c\right) \cos 2\omega_m^0 \cos 2\omega \ , \tag{A4}$$

$$P_1 = -\cos 2\omega_m^0 \sin 2\omega \sqrt{P_c(1-P_c)} \cos(\xi_v + \pi - \alpha - \beta) \ , \tag{A5}$$

$$P_2 = -\sin 2\omega_m^0 \cos 2\omega \sqrt{P_c(1-P_c)} \cos(\alpha - \beta) \ , \tag{A6}$$

$$P_3 = -\frac{1}{2} \sin 2\omega_m^0 \sin 2\omega P_c[\cos(\xi - 2\alpha) + \cos(\xi_v - 2\beta)] \ , \tag{A7}$$

$$P_4 = \frac{1}{2} \sin 2\omega_m^0 \sin 2\omega \cos(\xi_v - 2\alpha) \ . \tag{A8}$$

It has been shown in [21,22] that the last three terms $P_{2,3,4}$ can, in general, be safely neglected for practical purposes, so that one can take

$$P_{ee} = P_0 + P_1 \ , \tag{A9}$$

which, together with the identification

$$\xi_s = \pi - \beta - \alpha \ , \tag{A10}$$

leads to Eqs. (10)–(12).[16]

In the QVO regime relevant for our work ($k \lesssim 10^{-8}$ eV^2/MeV), the negligibility of $P_{2,3,4}$ is evident from the fact that $k/V(x_0) \lesssim 4 \times 10^{-3}$ for $x_0 \lesssim 0.25 R_\odot$, so that the $P_{2,3,4}$ prefactor $\sin 2\omega_m^0$ is negligibly small, while the nonvanishing terms $P_{0,1}$ can be written as:

$$P_0^{\rm QVO} \simeq \cos^2 \omega P_c + \sin^2 \omega (1 - P_c) \ , \tag{A11}$$

$$P_1^{\rm QVO} \simeq 2 \sin \omega \cos \omega \sqrt{P_c(1-P_c)} \cos \xi \ . \tag{A12}$$

It was shown in [27] that the above equations are not spoiled by Earth matter effects,[17] as they turn out to be negligible in the QVO range—a fortunate circumstance that considerably simplifies the calculations.

---

[16] One can make contact with the Φ_{ij} phase notation of [21,22,30] through the following identifications: $\Phi_{11} = -\alpha + \xi_v/2$; $\Phi_{12} = \beta - \xi_v/2$; $\Phi_{21} = \pi - \beta + \xi_v/2$; and $\Phi_{22} = \alpha - \xi_v/2$. The notation in the present work explicitly factorizes out the contribution of the vacuum phase ξ_v for $x \in [R_\odot, L]$.

[17] Equations (A11) and (A12) in this work coincide with Eq. (28) in [27], modulo the identification $P_\odot = P_c$, valid in the QVO regime.

We have verified the applicability of the approximations in Eq. (A11) and (A12) in the QVO regime, by checking that our exact results do not change in any appreciable way by setting $\cos\omega_m^0 \equiv 0$ from the start. In particular, the results of the numerical integration of the evolution equations vary very little by forcing the initial state to be ν_{2m} rather than ν_e. We have also verified that none of our figures changes in a graphically perceptible way in the QV range, by moving the point x_0 within the production zone ($x_0 \lesssim 0.25 R_\odot$) not only radially but also for off-center trajectories.[18] Therefore, in the following appendixes, we will neglect corrections of $O(k/V(x_0))$ in the QVO regime, and just set

$$x_0 \equiv 0 \ , \tag{A13}$$

$$\omega_m^0 \equiv \pi/2 \ , \tag{A14}$$

from the start, without any appreciable loss of accuracy.

Given Eq. (A2), and the fact that the initial state can be taken, to a high degree of accuracy, $\nu_e = \nu_{2m}$, the probability amplitudes to find the two mass eigenstates at $x = R_\odot$ ($\xi_v = 0$) simply read

$$A_{21} = \sqrt{P_c} e^{i(\pi-\beta)} \ , \tag{A15}$$

$$A_{22} = \sqrt{1-P_c} e^{i\alpha} \ . \tag{A16}$$

In terms of flavor state transition amplitudes A_{ee} and A_{ex} at $x = R_\odot$, the jump probability reads

$$P_c^{\rm QVO} = |A_{21}|^2 \ , \tag{A17}$$

$$= |A_{ee}|^2 \cos^2\omega + |A_{ex}|^2 \sin^2\omega - 2\,{\rm Re}(A_{ee}\,A_{ex}^*)\sin\omega\cos\omega \ , \tag{A18}$$

and the phase reads[19]

$$\xi_s^{\rm QVO} = \arg(A_{21}\,A_{22}^*) \tag{A19}$$

$$= \arg[\sin\omega\cos\omega(|A_{ee}|^2 - |A_{ex}|^2) + {\rm Re}(A_{ee}A_{ex}^*)\cos 2\omega + i\,{\rm Im}(A_{ee}A_{ex}^*)] \ . \tag{A20}$$

We conclude this Appendix by quoting useful expressions for some dimensionless quantities which appear in the calculation of P_c and ξ:

$$L/R_\odot = 215 \ , \tag{A21}$$

$$kR_\odot = 1.76\times 10^9 \left(\frac{\delta m^2/E}{{\rm eV}^2/{\rm MeV}}\right) \ , \tag{A22}$$

$$VR_\odot = 2.69\times 10^2 \left(\frac{N_e}{{\rm mol/cm}^3}\right) \ , \tag{A23}$$

$$V/k = 1.53\times 10^{-7} \left(\frac{\delta m^2/E}{{\rm eV}^2/{\rm MeV}}\right)^{-1} \left(\frac{N_e}{{\rm mol/cm}^3}\right) \ . \tag{A24}$$

---

[18] Notice that the x_0-independence of $P_{ee}^{\rm QVO}$ implies that no smearing over the production zone is necessary, as also emphasized in [27].

[19] Equations (A18) and (A20) can also be obtained from Eqs. (13a)–(13d), (15), and (19) in [30].

APPENDIX B: THE CONDITION OF MAXIMAL VIOLATION OF ADIABATICITY

In this Appendix we characterize the condition of maximum violation of adiabaticity along the neutrino trajectory. We also show that the MVA condition reduces to the familiar resonance condition in appropriate limits.

In the matter eigenstate basis, the neutrino evolution equation

$$i\frac{d}{dx}\begin{pmatrix}\nu_{1m}\\ \nu_{2m}\end{pmatrix} = H'\begin{pmatrix}\nu_{1m}\\ \nu_{2m}\end{pmatrix} \ , \tag{B1}$$

is governed by the Hamiltonian

$$H' = \frac{k_m}{2}\begin{pmatrix}-1 & -2\,i\,\dot{\omega}_m/k_m\\ 2\,i\,\dot{\omega}_m/k_m & 1\end{pmatrix} \ . \tag{B2}$$

where $\dot{\omega}_m = d\omega_m/dx$.

The evolution is adiabatic when the diagonal term dominates over the off-diagonal term, so that the ratio of such elements [the function $\gamma(x)$ defined in Eq. (32)] is large. The "maximal violation of adiabaticity" along the neutrino trajectory is reached at the point $x = x_{\rm mva}$ where $\gamma(x)$ is instead minimized,

$$\frac{d\gamma(x)}{dx} = 0 \ \leftrightarrow \ x = x_{\rm mva} \ . \tag{B3}$$

The above MVA condition can be rewritten as

$$\frac{d^2\cos 2\omega_m}{dx^2} = 0 \ \leftrightarrow \ x = x_{\rm mva} \ . \tag{B4}$$

Since $\cos 2\omega_m$ increases monotonically from its value at the production point ($\simeq -1$) to its vacuum value ($\cos 2\omega$), the above condition characterizes the (flex) point of fastest increase for the function $\cos 2\omega_m(x)$, which is thus uniquely defined at any $\omega \in [0, \pi/2]$.

The MVA condition (B4) can be compared with the usual resonance condition,

$$\cos 2\omega_m = 0 \ \leftrightarrow \ x = x_{\rm res} \ . \tag{B5}$$

which can be fulfilled only for $\omega \in [0, \pi/4]$. To understand under which circumstances the two conditions practically coincide ($x_{\rm mva} \simeq x_{\rm res}$), it is useful to rewrite the MVA condition in the following, equivalent form:

$$3\sin 2\omega_m \cos 2\omega_m (\dot{V})^2 + k \sin 2\omega \ddot{V} = 0 \ \leftrightarrow \ x = x_{\rm mva} \ . \tag{B6}$$

The above condition reduces to Eq. (B5) in the case linear density ($\ddot{V} = 0$) (which, however, is not applicable to the Sun). It also reduces to Eq. (B5) for very small mixing ($\sin 2\omega \to 0$), which explains why the simple resonance condition has been very frequently used in the literature, to replace the slightly more complicated MVA condition. Notice also that, for increasing k, P_c becomes nonnegligible only at small mixing angles. Therefore, as far as the

calculation of P_c is concerned, the MVA and resonance conditions also merge at large k. In all other cases, it turns out that $x_{\rm res} > x_{\rm mva}$ for $\omega \in [0, \pi/4]$. For $\omega \in [\pi/4, \pi/2]$, $x_{\rm res}$ is simply not defined.

We conclude by providing a handy approximation to the value of $x_{\rm mva}$, which may be used to by-pass the calculation of derivatives of $V(x)$, at the price of a small loss of accuracy in the calculation of P_{ee}. As discussed before, the MVA condition characterizes the flex point of the curve $\cos\omega_m(x)$, which increases from -1 to $\cos 2\omega$ in the QVO range. We have verified that, in the parameter region where P_c is nonnegligible, the flex point $x_{\rm mva}$ is close to the half-rise point $x_{1/2}$ where $\cos 2\omega_m$ assumes the average value between its two extrema, defined as

$$\cos 2\omega_m(x_{1/2}) \equiv \frac{1}{2}(\cos 2\omega - 1) \ . \tag{B7}$$

The above definition leads to the condition

$$V(x_{1/2}) = k\cos 2\omega + \frac{k\sin^3\omega}{\sqrt{1+\sin^2\omega}} \ , \tag{B8}$$

which clearly reduces to the resonance condition in the small ω limit. Using $r_0(x_{1/2})$ as a substitute for $r_0(x_{\rm mva})$ in the MVA prescription [Eq. (37)] provides a final accuracy of $\lesssim 4.5\times 10^{-2}$ in P_{ee} in the whole QV regime (only slightly worse than the accuracy quoted at the end of Sec. VII).

APPENDIX C: EXPANSION OF P_c AT FIRST ORDER IN k

In this Appendix we study the limit $k \to 0$ for P_c, in both cases of exponential and SSM density. Such limit gives an asymptotic value for the effective scale parameter r_0, relevant for the lower part of the QV regime. The positions in Eqs. (A13) and (A14) are adopted. We also introduce a normalized radial coordinate,

$$\rho = x/R_\odot \ . \tag{C1}$$

In the case of exponential density, Eq. (22) gives, at first order in k,

$$P_c = \cos^2\omega - \frac{\pi}{4}\, r_0\, k \sin^2 2\omega \ , \tag{C2}$$

where $r_0 = R_\odot/10.54$ [Eq. (19)].

In the case of SSM density, we demonstrate that Eq. (C2) is formally preserved, modulo the replacement

$$r_0 \to r_0' = R_\odot/18.9 \ . \tag{C3}$$

The crucial observation is that, for $k \lesssim 10^{-9}$ eV^2/MeV and SSM density, we have $k \ll V(x)$ for most of the ν trajectory inside the Sun ($\rho \lesssim 0.9$) before the rapid density drop at the border. This suggest a perturbative solution of Eqs. (1) and (2) with the vacuum term H_v playing the role of a small perturbation, as compared with the dominant matter term H_m.

The perturbative expansion is expected to be accurate when the second term in Eq. (C2) is small, namely, for $kr_0 \ll 1$.

At 0th order in H_v, the evolution operator from $\rho = 0$ to $\rho = 1$ is trivial in the flavor basis (H_m being diagonal),

$$T_0(1,0) = \exp\left(-i\int_0^1 d\rho\, H_m(\rho)\right) \tag{C4}$$

$$= \begin{pmatrix} \exp\left[-\frac{i}{2}\eta(1,0)\right] & 0 \\ 0 & \exp\left[+\frac{i}{2}\eta(1,0)\right] \end{pmatrix} , \tag{C5}$$

where

$$\eta(\rho_2,\rho_1) = \int_{\rho_1}^{\rho_2} d\rho\, V(\rho) R_\odot \ . \tag{C6}$$

At 1st order in H_v (i.e., in k), one gets an improved evolution operator T_1,

$$T_1(1,0) = T_0(1,0)[\mathbf{1} - i\Delta(1,0)] \ , \tag{C7}$$

where the correction matrix Δ reads

$$\Delta(1,0) = T_0^{-1}(1,0)\int_0^1 d\rho\, T_0(1,\rho)\, H_v\, T_0(\rho,0) \tag{C8}$$

$$= \frac{kR_\odot}{2}\begin{pmatrix} -\cos 2\omega & \sin 2\omega \int_0^1 d\rho\, e^{i\eta(\rho,0)} \\ \sin 2\omega \int_0^1 d\rho\, e^{-i\eta(\rho,0)} & \cos 2\omega \end{pmatrix} . \tag{C9}$$

By applying T_1 to the initial flavor state $\psi_e = (1,0)^T$, one gets the flavor state at $x = R_\odot$,

$$\begin{pmatrix} \nu_e \\ \nu_x \end{pmatrix}_{R_\odot} = e^{-\frac{i}{2}\eta(1,0)}\left[\begin{pmatrix} 1 \\ 0 \end{pmatrix} - \frac{i}{2}kR_\odot \begin{pmatrix} -\cos 2\omega \\ \sin 2\omega \int_0^1 d\rho\, e^{i\eta(1,\rho)} \end{pmatrix}\right] , \tag{C10}$$

where the $O(k)$ correction is explicited. The basic integral,

$$I_\eta = \int_0^1 d\rho \exp[i\,\eta(1,\rho)] = C + iS \ , \tag{C11}$$

appearing in Eq. (C10), can be numerically evaluated using the SSM density,

$$C = \int_0^1 d\rho\, \cos\int_\rho^1 d\rho' V(\rho') R_\odot = 0.1303 \ , \tag{C12}$$

$$S = \int_0^1 d\rho\, \sin\int_\rho^1 d\rho' V(\rho') R_\odot = 0.0832 \ . \tag{C13}$$

Finally, using Eqs. (A18,C10) and keeping only $O(k)$ terms, one gets

$$P_c \simeq \cos^2\omega - \sin 2\omega\, \mathrm{Re}(\nu_e \nu_x^*) \tag{C14}$$

$$\simeq \cos^2\omega - \frac{1}{2}kR_\odot S \sin^2 2\omega \ , \tag{C15}$$

which reproduces Eq. (C2), up to the anticipated replacement

$$r_0 \to r_0' = 2\,S\,R_\odot/\pi = R_\odot/18.9\ . \tag{C16}$$

We have independently checked the value $r_0' = R_\odot/18.9$ by numerical studies of the $k \to 0$ limit for the quantity $(P_c - \cos^2\omega)/k$, with P_c derived exactly rather than perturbatively.[20]

We observe that, for the SSM density, the scale parameter $r_0(x)$ happens to be equal to the value in Eq. (C3) at $x = 0.904\,R_\odot$,

$$r_0(0.904\,R_\odot) = R_\odot/18.9 = r_0'\ . \tag{C17}$$

Such relation proves useful to match our analytical and perturbative results around the critical zone of the "knee" of the SSM density, which occurs just at $x \simeq 0.9 R_\odot$.

As a final exercise, we prove that $r_0' \simeq r_0$ in the exponential limit $V(x) = V(0)e^{-x/r_0}$, as it should be. The proof uses the assumptions of large initial density and small final density, as discussed for Eqs. (20) and (21). Then one changes the integration variable from ρ to $\phi = V(0) r_0 e^{-\rho R_\odot/r_0}$ in the calculation of S [Eq. (C13)], and exploits the fact that ϕ is very small (large) for $\rho = 1$ ($\rho = 0$):

$$\frac{r_0'}{R_\odot} = \frac{2}{\pi}\int_0^1 d\rho\,\sin\int_\rho^1 d\rho'\,V(0)\,R_\odot\,e^{-\rho' R_\odot/r_0} \tag{C18}$$

$$\simeq \frac{2}{\pi}\int_0^1 d\rho\,\sin\left(V(0)\,r_0\,e^{-\rho R_\odot/r_0}\right) \tag{C19}$$

$$\simeq \frac{r_0}{R_\odot}\frac{2}{\pi}\int_0^\infty d\phi\,\frac{\sin\phi}{\phi} = \frac{r_0}{R_\odot}\ . \tag{C20}$$

APPENDIX D: EXPANSION OF ξ_s AT FIRST ORDER IN k

In this Appendix we study the small-k limit of the phase ξ_s, by using the same strategy adopted in the previous section for P_c. In particular, let us consider the $O(k)$ expansion of the analytical phase in Eq. (23),

$$\xi_s \simeq k\,R_\odot\,C'\ , \tag{D1}$$

where[21]

$$C' = 1 - \frac{r_0}{R_\odot}[\gamma_E + \ln r_0 V(0)] = 0.116\ . \tag{D2}$$

---

[20] The author of [25,36] found numerically a similar value for r_0' (namely, $R_\odot/18.4$), by fitting his exact results for small k. In this Appendix we have given an explicit derivation of r_0', based on perturbation theory, and independent on numerical fits.

[21] $\gamma_E \simeq 0.577$ is the Euler constant.

We show that Eq. (D1), valid for exponential density, remains formally unchanged also for the SSM density, modulo the replacement $C' \to C$, where $C = 0.130$ is given by Eq. (C12). In fact, using Eqs. (A20) and (C10), and keeping only the $O(k)$ terms, we get

$$\xi_s \simeq 2\mathrm{Im}(A_{ee}A_{ex}^*)/\sin 2\omega \tag{D3}$$
$$= k\,R_\odot\,C\ . \tag{D4}$$

Such result is independently confirmed by studying the $k \to 0$ limit of the quantity $\xi_s/kR_\odot$, with ξ_s derived from exact (rather than perturbative) calculations.

Finally, we show that $C \simeq C'$ in the limit of exponential density, as it should be. With manipulations similar to those used to derive Eq. (C20) we get:

$$C = \int_0^1 d\rho\,\cos\int_\rho^1 d\rho'\,V(0)\,R_\odot\,e^{-\rho' R_\odot/r_0} \tag{D5}$$
$$\simeq \int_0^1 d\rho\,\cos\left(V(0)\,r_0\,e^{-\rho R_\odot/r_0}\right) \tag{D6}$$
$$= 1 - \int_0^1 d\rho\,\left[1-\cos\left(V(0)\,r_0\,e^{-\rho R_\odot/r_0}\right)\right] \tag{D7}$$
$$= 1 - \frac{r_0}{R_\odot}\int_0^{r_0V(0)}\frac{1-\cos\phi}{\phi} \tag{D8}$$
$$\simeq 1 - \frac{r_0}{R_\odot}[\gamma_E + \ln r_0V(0)] = C' \tag{D9}$$

where, in the divergent integral of Eq. (D8), we have kept only the two leading terms [γ_E and $\ln r_0V(0)$] which do not decrease when the upper limit $r_0V(0)$ becomes large.

APPENDIX E: EXPANSION OF ξ_s AT SECOND ORDER IN k

In this Appendix, we present an $O(k^2)$ perturbative expression for ξ_s, which effectively accounts for the ω-dependence of the exact results (as evident in the upper part of the QVO range in Fig. 9).

We basically iterate the calculation of the evolution operator $T(1,0)$ (see Appendix C) at second order in the perturbation term H_v. We omit the (somewhat lengthy) derivation and present the final $O(k^2)$ result,

$$\xi_s = (kR_\odot)\,\mathrm{Re}I_\eta + (kR_\odot)^2\,\cos 2\omega\,[\mathrm{Im}(I_\eta - I'_\eta + I''_\eta)/2 - \mathrm{Re}I_\eta\cdot\mathrm{Im}I_\eta] \tag{E1}$$
$$= 0.130\,(kR_\odot) + 1.67\times10^{-3}(kR_\odot)^2\,\cos 2\omega\ , \tag{E2}$$

where $I_\eta = (13.03 + i\,8.32)\times10^{-2}$ is defined in Eq. (C11), while I'_η and I''_η are defined as

$$I'_\eta = \int_0^1 d\rho\,\rho\,\exp[i\,\eta(1,\rho)] \tag{E3}$$
$$= (12.45 + i\,7.07)\times10^{-2}\ , \tag{E4}$$
$$I''_\eta = \int_0^1 d\rho\int_0^\rho d\rho'\,\exp[i\,\eta(1,\rho')] \tag{E5}$$
$$= (0.58 + i\,1.25)\times10^{-2}\ , \tag{E6}$$

and have been numerically evaluated for SSM density. The $O(k)$ term reproduces, of course, the results given in the previous section.

The $O(k^2)$ behavior of Eq. (E2) is not captured by the analytical phase written in the form of Eq. (23), which contains only odd powers in a k-expansion. The reason can be traced to the fact that Eq. (23) was derived in [21,30] under the assumption of zero density at $x = R_\odot$ (which is not exactly fulfilled for exponential density). Preliminary studies indicate that removal of such assumption gives the correct $O(k^2)$ behavior of the analytical phase [including the $\cos 2\omega$ dependence displayed in Eq. (E2)]. Such studies are proceeding and will be presented after completion.

REFERENCES

[1] J.N. Bahcall, *Neutrino Astrophysics* (Cambridge University Press, Cambridge, England, 1989).

[2] Homestake Collaboration, B.T. Cleveland, T.J. Daily, R. Davis Jr., J.R. Distel, K. Lande, C. K. Lee, P.S. Wildenhain, and J. Ullman, Astrophys. J. **496**, 505 (1998).

[3] Kamiokande Collaboration, Y. Fukuda *et al.*, Phys. Rev. Lett. **77**, 1683 (1996).

[4] SAGE Collaboration, J.N. Abdurashitov *et al.*, Phys. Rev. C **60**, 055801 (1999).

[5] GALLEX Collaboration, W. Hampel *et al.*, Phys. Lett. B **447**, 127 (1999).

[6] SuperKamiokande Collaboration, Y. Fukuda *et al.*, Phys. Rev. Lett. **82**, 2430 (1999).

[7] SuperKamiokande Collaboration, talk by Y. Suzuki in *Neutrino 2000*, 19th International Conference on Neutrino Physics and Astrophysics (Sudbury, Canada, 2000), to appear in the Proceedings.

[8] GNO Collaboration, M. Altmann *et al.*, Phys. Lett. B **490**, 16 (2000).

[9] J.N. Bahcall, M.H. Pinsonneault, and S. Basu, astro-ph/0010346.

[10] J.N. Bahcall homepage, http://www.sns.ias.edu/~jnb (Neutrino Software and Data).

[11] B. Pontecorvo, Zh. Eksp. Teor. Fiz. **53**, 1717 (1967) [Sov. Phys. JETP **26**, 984 (1968)]; Z. Maki, M. Nakagawa, and S. Sakata, Prog. Theor. Phys. **28**, 675 (1962); V. Gribov and B. Pontecorvo, Phys. Lett. B **28**, 493 (1969).

[12] L. Wolfenstein, Phys. Rev. D **17**, 2369 (1978).

[13] S.P. Mikheyev and A.Yu. Smirnov, Yad. Fiz. **42**, 1441 (1985) [Sov. J. Nucl. Phys. **42**, 913 (1985)]; Nuovo Cimento C **9**, 17 (1986).

[14] V. Barger, S. Pakvasa, R.J.N. Phillips and K. Whisnant, Phys. Rev. D **22**, 2718 (1980).

[15] S.M. Bilenky, C. Giunti, and W. Grimus, Prog. Part. Nucl. Phys. **43**, 1 (1999).

[16] J.N. Bahcall, P.I. Krastev, and A.Yu. Smirnov, Phys. Rev. D **58**, 096016 (1998).

[17] Talks by D. Montanino and by A. Palazzo at *NOW 2000*, 2nd Europhysics Neutrino Oscillation Workshop (Conca Specchiulla, Italy, 2000), to appear in the Proceedings. Transparencies available at http://www.ba.infn.it/~now2000

[18] M.C. Gonzalez-Garcia, M. Maltoni, C. Peña-Garay, and J.W.F. Valle, hep-ph/0009350.

[19] S.M. Bilenky and S.T. Petcov, Rev. Mod. Phys. **59**, 671 (1987).

[20] S.T. Petcov, Phys. Lett. B **200**, 373 (1988).

[21] S.T. Petcov, Phys. Lett. B **214**, 139 (1988).

[22] S.T. Petcov and J. Rich, Phys. Lett. B **224**, 426 (1989).

[23] J. Pantaleone, Phys. Lett. B **251**, 618 (1990).

[24] S. Pakvasa and J. Pantaleone, Phys. Rev. Lett. **65**, 2479 (1990).

[25] A. Friedland, Phys. Rev. Lett. **85**, 936 (2000).

[26] A. de Gouvêa, A. Friedland, and H. Murayama, Phys. Lett. B **490**, 125 (2000).

[27] G.L. Fogli, E. Lisi, D. Montanino, and A. Palazzo, Phys. Rev. D **62**, 113004 (2000).

[28] A.M. Gago, H. Nunokawa, and R. Zukanovich Funchal, hep-ph/0007270.

[29] See, e.g., V. Barger, K. Whisnant, and R.J.N. Phillips, Phys. Rev. D **24**, 538 (1981); S.L. Glashow and L.M. Krauss, Phys. Lett. B **190**, 199 (1987); A. Acker, S. Pakvasa, and J. Pantaleone, Phys. Rev. D 43, 1754 (1991); P.I. Krastev and S.T. Petcov, Phys. Lett. B **285**, 85 (1992) and *ibid.* B **299**, 99 (1993); N. Hata and P. Langacker, Phys. Rev. D **56**, 6107 (1997); B. Faïd, G.L. Fogli, E. Lisi, and D. Montanino, Astropart. Phys. **10**, 93 (1999).

[30] S.T. Petcov, Phys. Lett. B **406**, 355 (1997).
[31] S. Toshev, Phys. Lett. B **196**, 170 (1987).
[32] M. Ito, T. Kaneko, and M. Nakagawa, Prog. Theor. Phys. **79**, 13 (1988); *erratum* **79**, 555 (1988).
[33] A. Abada and S.T. Petcov, Phys. Lett. B **279**, 153 (1992).
[34] M. Bruggen, W.C. Haxton and Y.-Z. Quian, Phys. Rev. D **51**, 4028 (1995).
[35] P.I. Krastev and S.T. Petcov, Phys. Lett. B **207**, 64 (1988); *erratum*, **214**, 661 (1988).
[36] A. Friedland, hep-ph/0010231.
[37] A. de Gouvea, A. Friedland, and H. Murayama, hep-ph/9910286.
[38] T.T. Kuo and J. Pantaleone, Rev. Mod. Phys. **61**, 937 (1989).
[39] G.L. Fogli, E. Lisi, and D. Montanino, Phys. Rev. D **54**, 2048 (1996).
[40] J.N. Bahcall and R. Ulrich, Rev. Mod. Phys. **60**, 297 (1988).
[41] S.P. Mikheyev and A.Yu. Smirnov, in *Moriond '87*, Proceedings of the 7th Moriond Workshop on New and Exotic Phenomena (Les Arcs, France, 1987), edited by O. Fackler and J. Trân Thanh Vân (Editions Frontières, Gif-sur-Yvette, France, 1987), p. 405.
[42] V. Barger, R.J.N. Phillips, and K. Whisnant, Phys. Rev. D **34**, 980 (1986).
[43] A. Messiah, in *Moriond '86*, Proceedings of the 6th Moriond Workshop on Massive Neutrinos in Astrophysics and in Particle Physics (Tignes, France, 1986), edited by O. Fackler and J. Trân Thanh Vân (Editions Frontières, Gif-sur-Yvette, France, 1986), p. 373.
[44] J. Pantaleone, Phys. Rev. D **43**, 2636 (1991).
[45] J.N. Bahcall and S.C. Frautschi, Phys. Lett. **29B**, 623 (1969).
[46] S.M. Bilenky and B. Pontecorvo, Phys. Rep. **41**, 225 (1978).
[47] See A.S. Dighe, Q.Y. Liu, and A.Yu. Smirnov, hep-ph/9903329, and references therein.
[48] J.N. Bahcall, Phys. Rev. D **49**, 3923 (1994).
[49] L. Krauss and F. Wilczek, Phys. Rev. Lett. **55**, 122 (1985).
[50] Borexino Collaboration, talk by G. Ranucci at *Neutrino 2000* [7].
[51] KamLAND Collaboration, talk by A. Piepke at *Neutrino 2000* [7].
[52] A. de Gouvêa, A. Friedland, and H. Murayama, Phys. Rev. D **60**, 093011 (1999).
[53] A.J. Baltz and J. Weneser, Phys. Rev. D **37**, 3364 (1988).

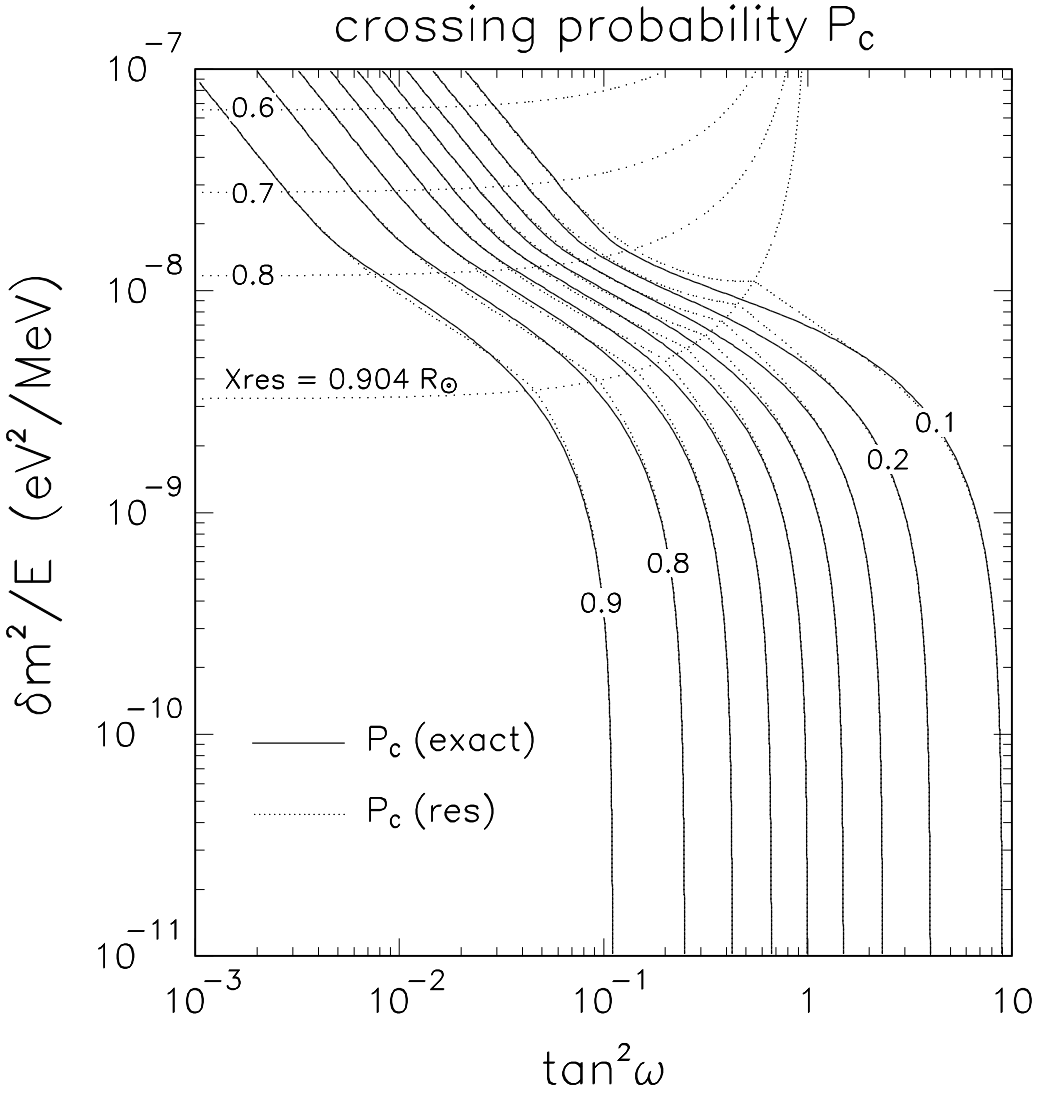

FIG. 1. The crossing probability P_c, calculated for the SSM density in the parameter space ($\delta m^2/E$, $\tan^2\omega$). The three lowest decades in $\delta m^2/E$ characterize the quasivacuum oscillation regime. Solid curves: exact numerical results. Dotted curves: approximate results, using the analytical resonance prescription. Also shown are isolines of resonance radii. The radius $x/R_\odot = 0.904$ represents the matching point of the resonance prescription with the perturbative results valid for small values of $\delta m^2/E$.

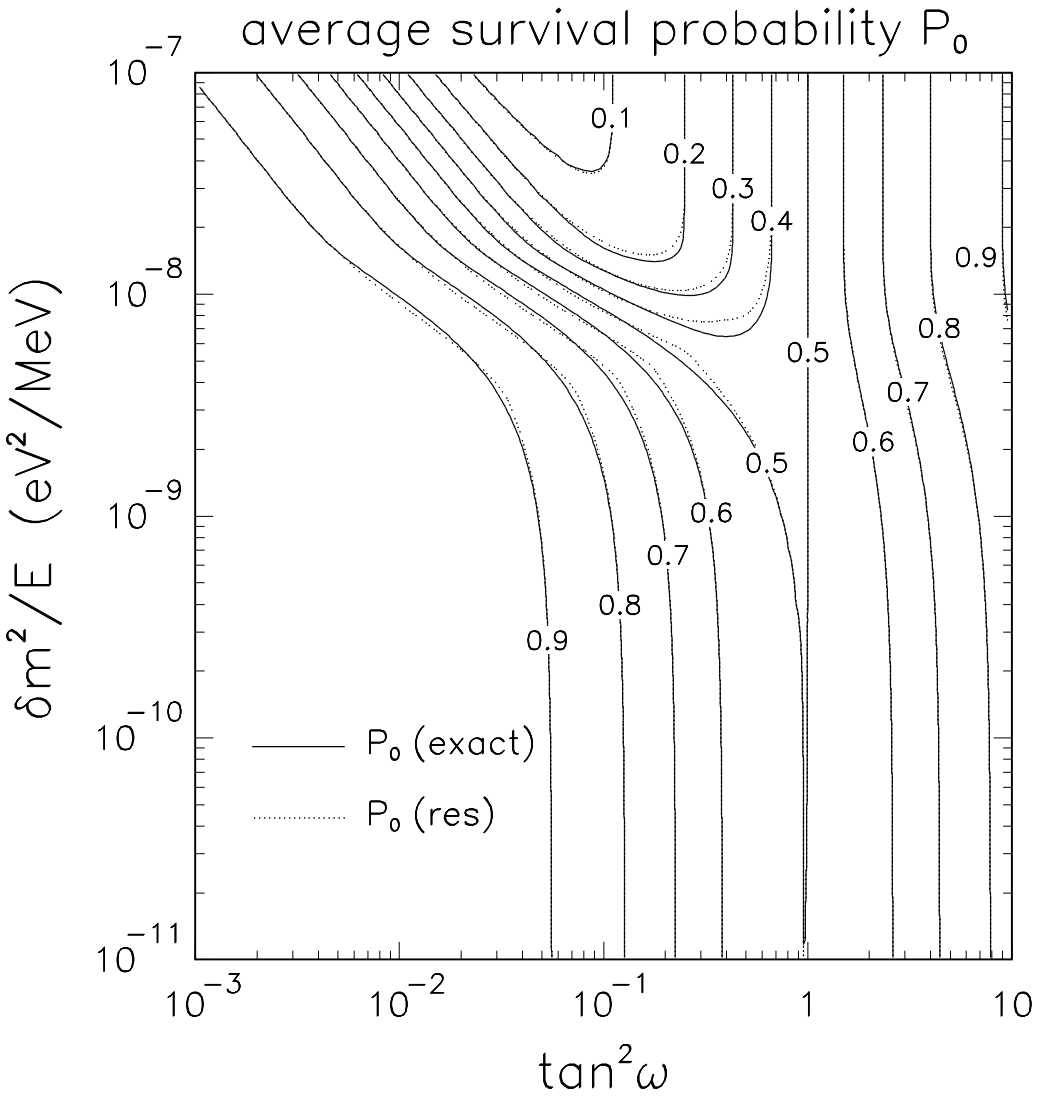

FIG. 2. The average survival probability P_0, as obtained through exact numerical calculations (solid curves) and through the analytical resonance prescription (dotted curves).

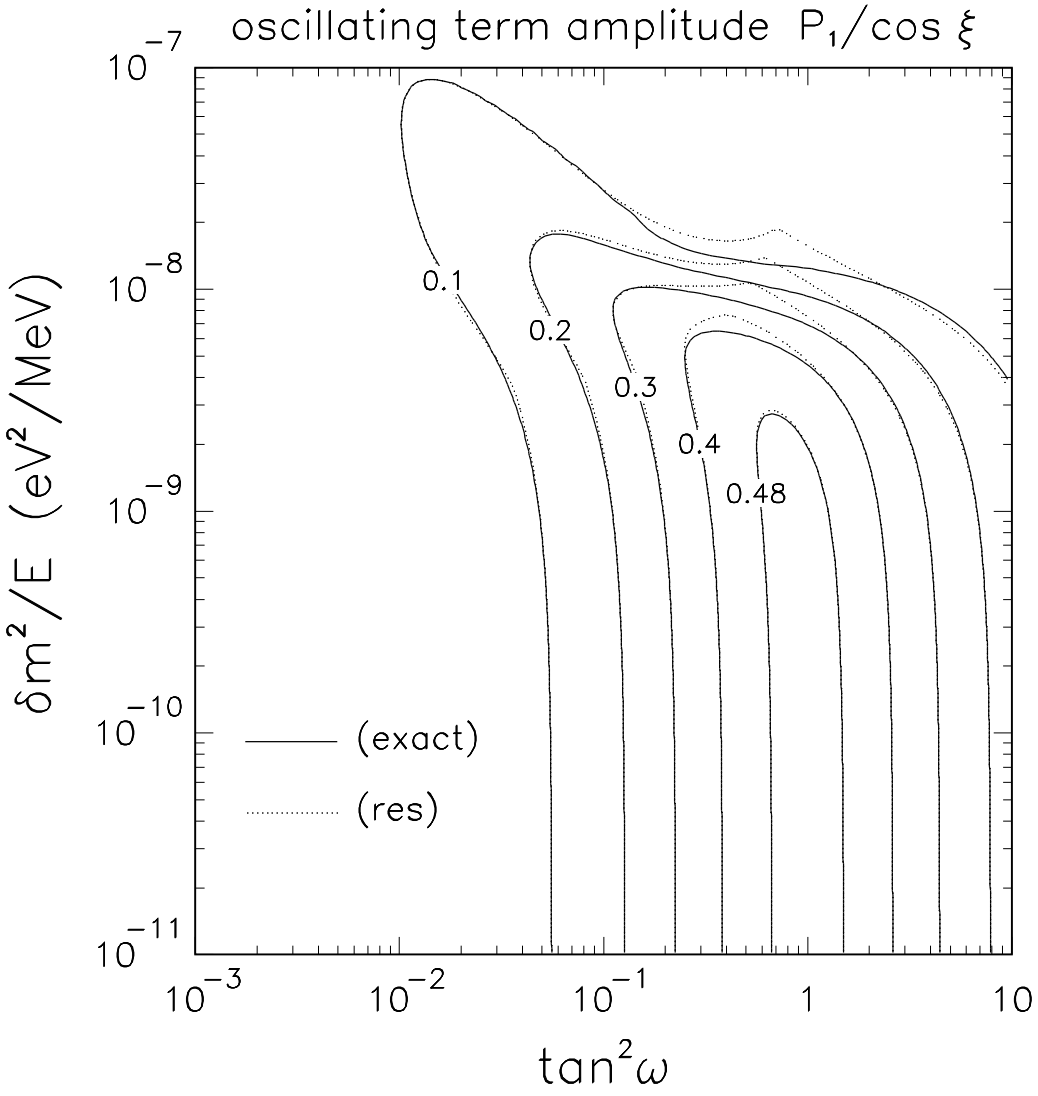

FIG. 3. The oscillating term prefactor $P_1/\cos\xi$, as obtained through exact numerical calculations (solid curves) and through the analytical resonance prescription (dotted curves).

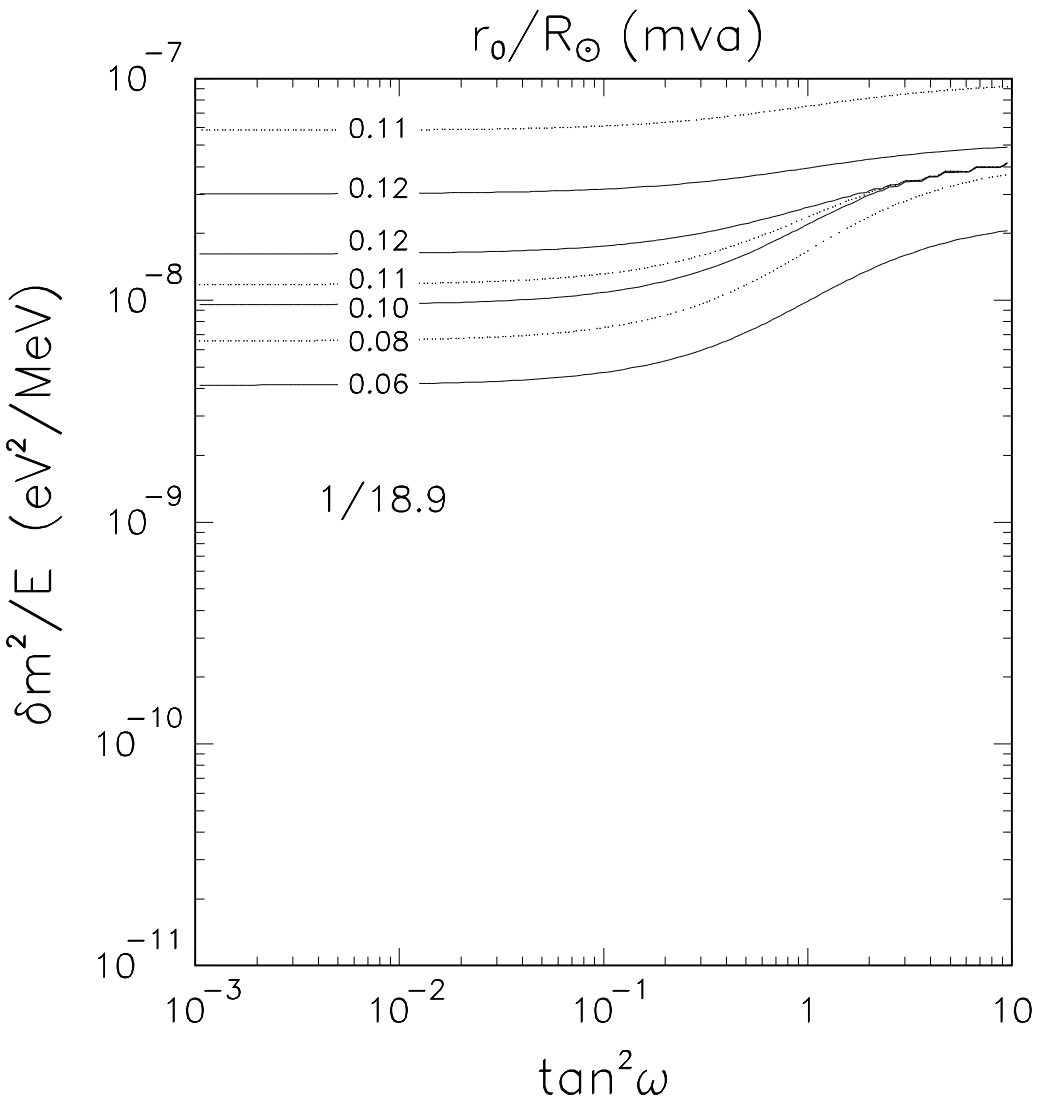

FIG. 4. Isolines of the effective density scale parameter r_0 (in units of $R_\odot$), as derived through the prescription of maximum violation of adiabaticity (MVA), matched with the perturbative result valid at small values of $\delta m^2/E$ ($r_0/R_\odot \to 1/18.9$).

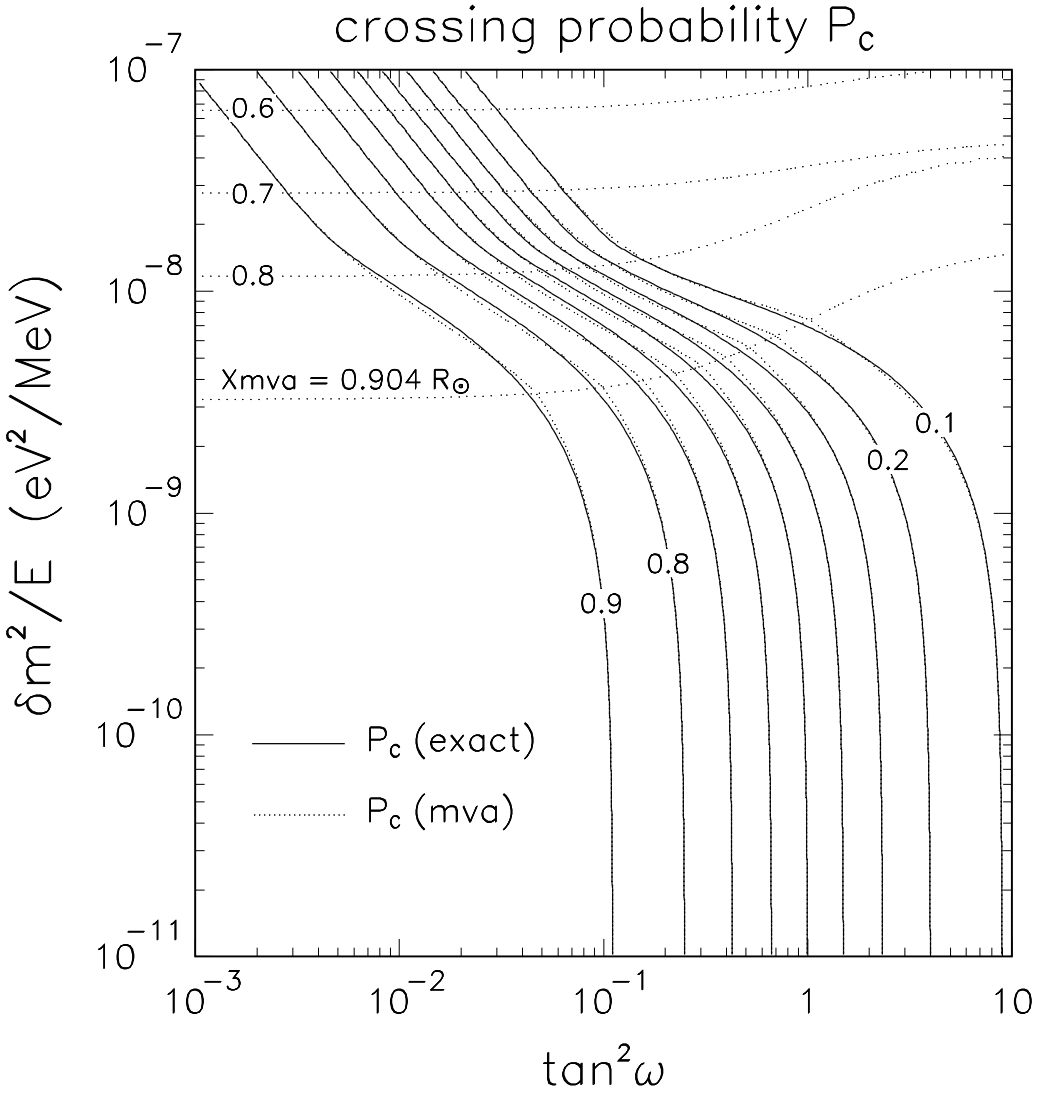

FIG. 5. The crossing probability P_c, as obtained through exact numerical calculations (solid curves) and through the analytical MVA prescription (dotted curves). Also shown are isolines of MVA radii. The radius $x/R_\odot = 0.904$ represents the matching point of the MVA prescription with the perturbative results valid at small values of $\delta m^2/E$.

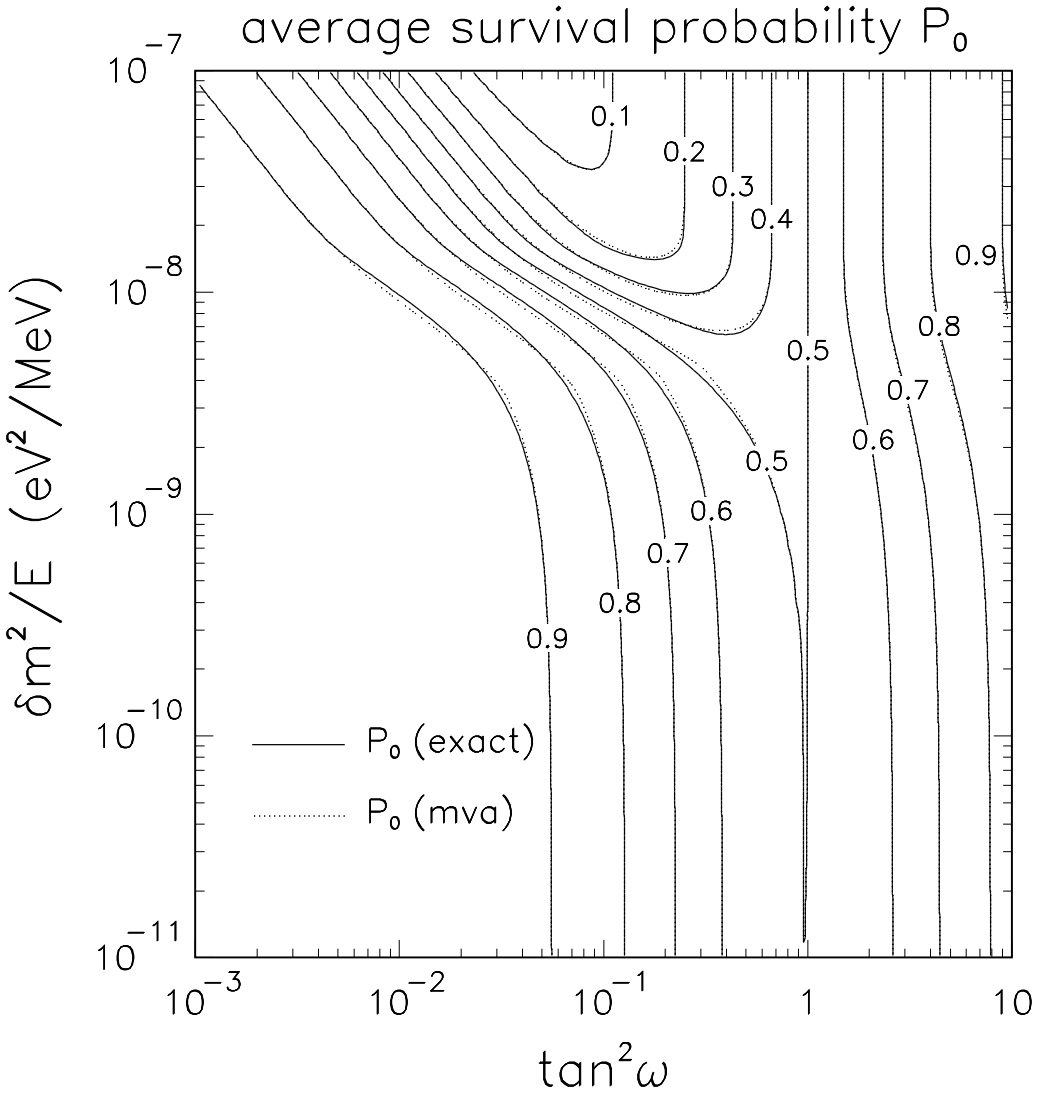

FIG. 6. The average survival probability P_0, as obtained through exact numerical calculations (solid curves) and through the analytical MVA prescription (dotted curves).

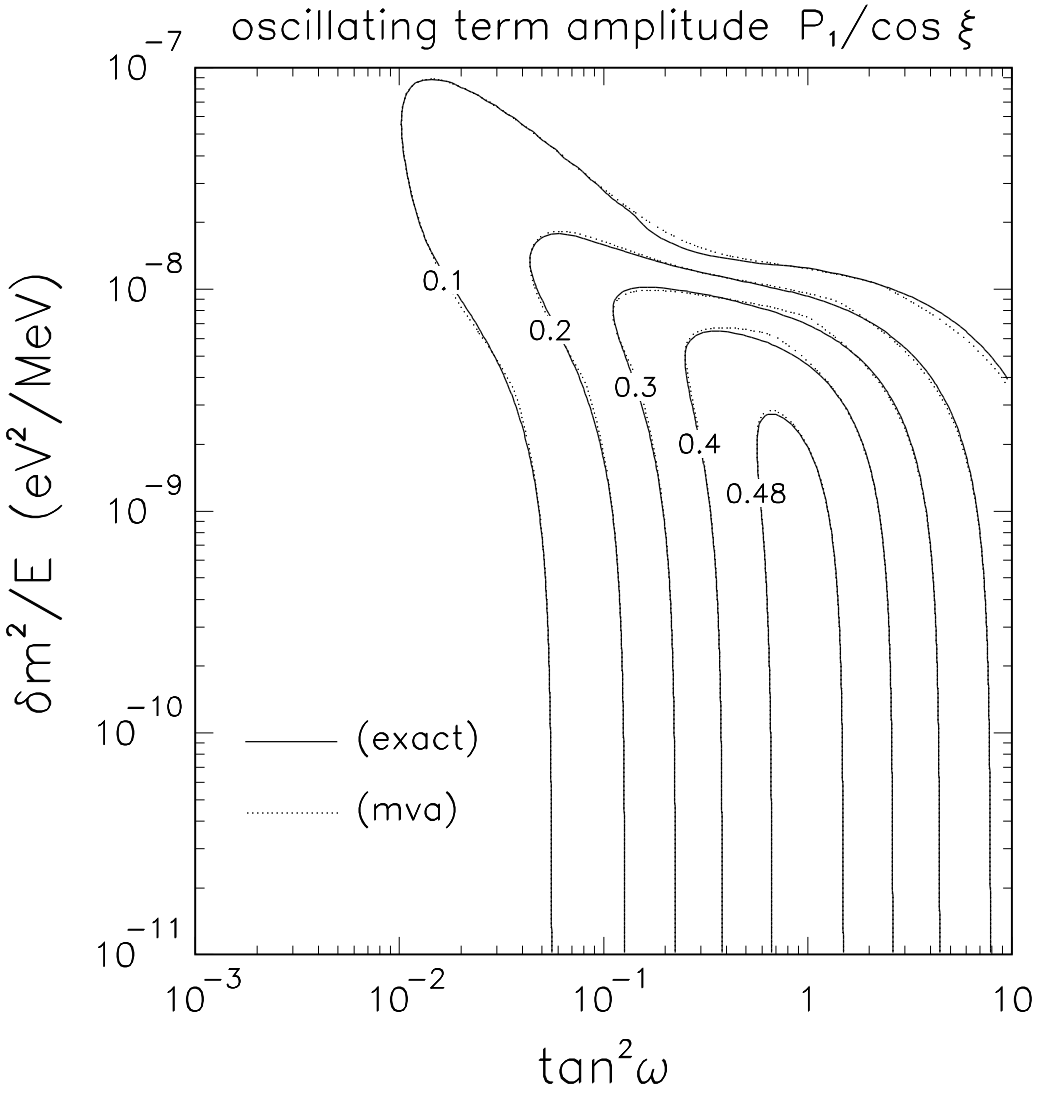

FIG. 7. The oscillating term prefactor $P_1/\cos\xi$, as obtained through exact numerical calculations (solid curves) and through the analytical MVA prescription (dotted curves).

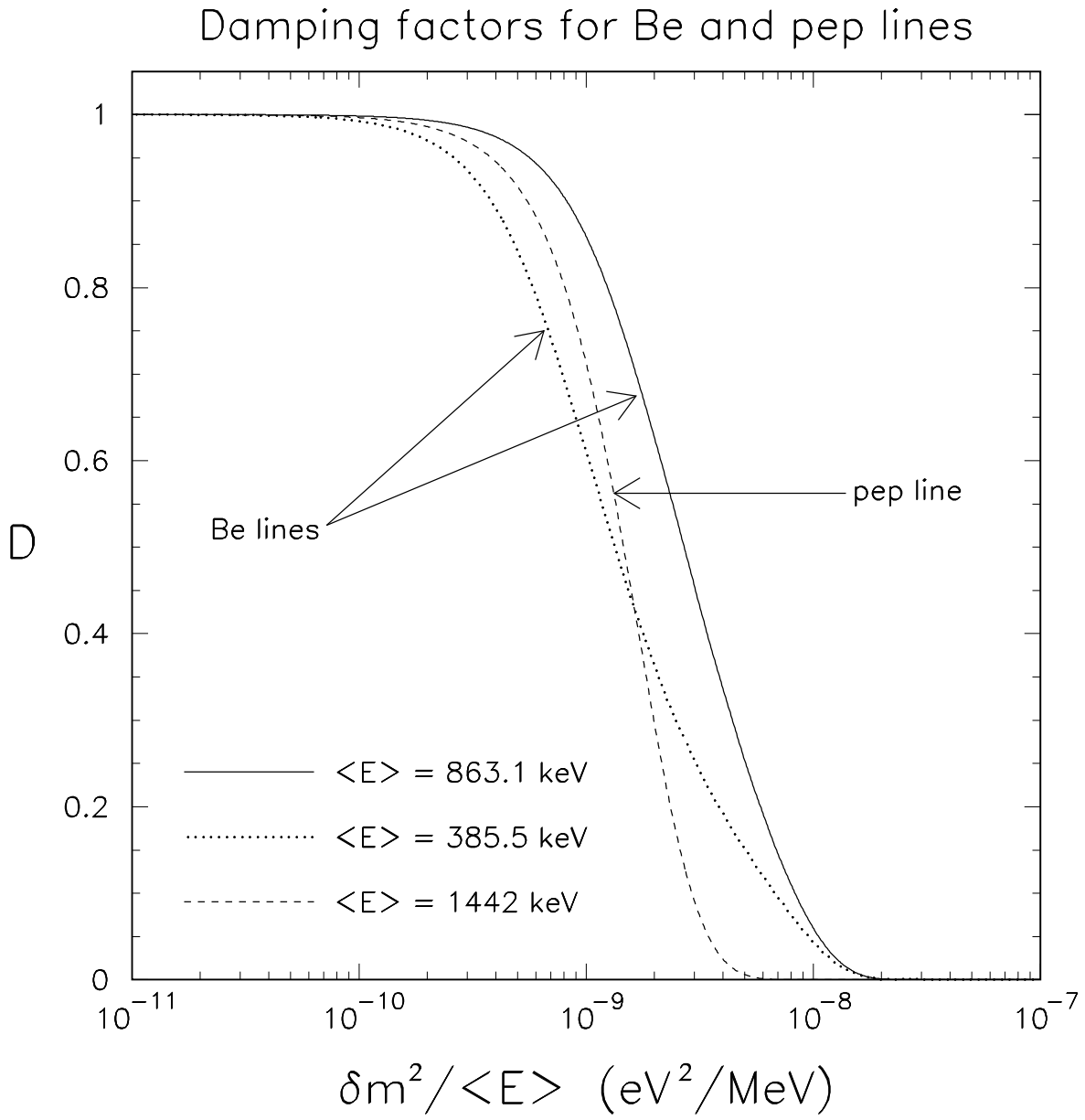

FIG. 8. Damping factors for the oscillating term $\cos\xi$, as calculated for the Be and *pep* solar neutrino lines ($\langle E\rangle$ being their average energy). The damping factors completely suppress oscillations at the Earth for $\delta m^2/\langle E\rangle$ above the quasivacuum range.

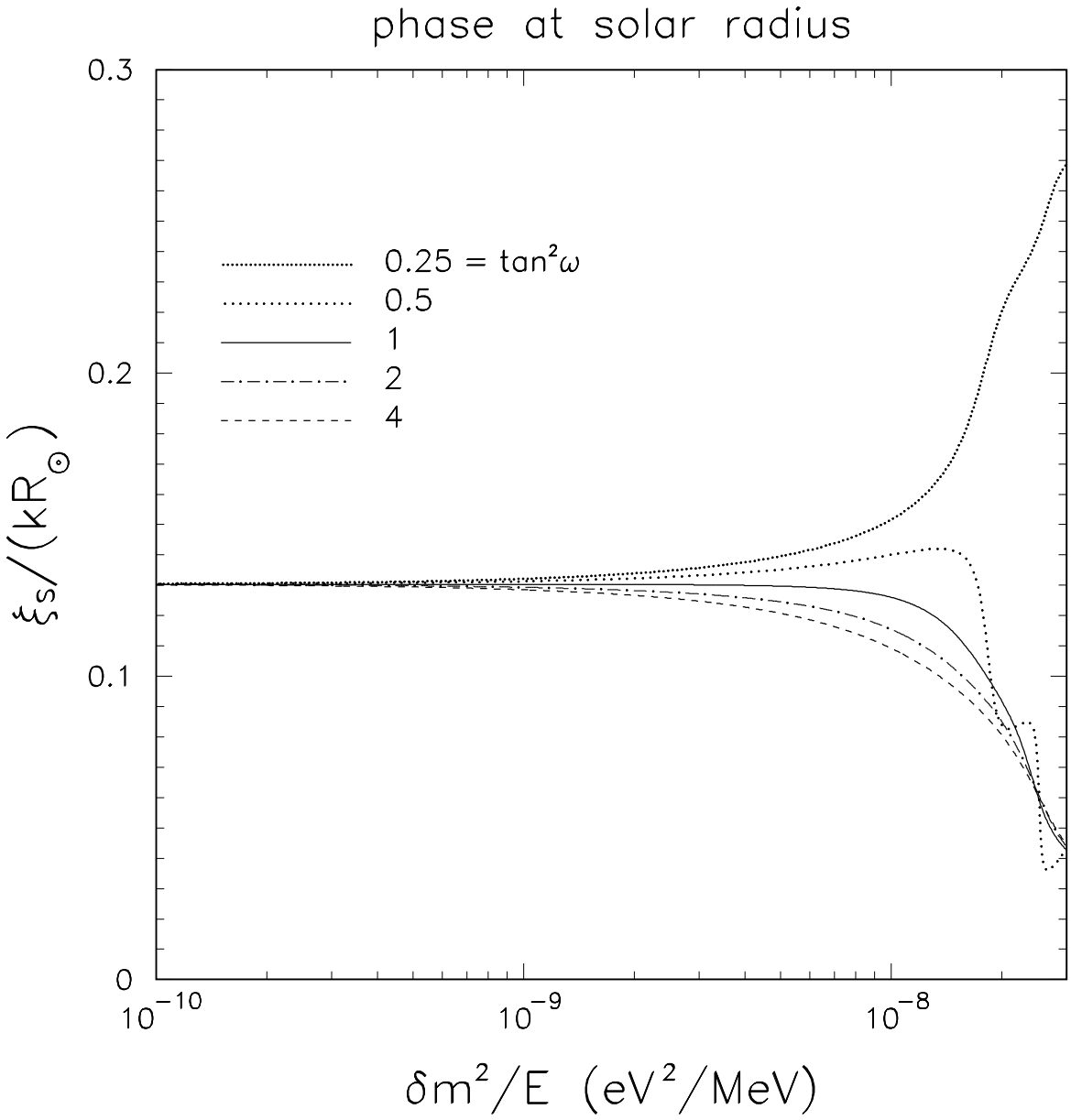

FIG. 9. The solar phase ξ_s, in units of $kR_\odot$, as obtained from exact numerical calculations for some representative values of ω. Notice the ω-independent limit for $k \to 0$.

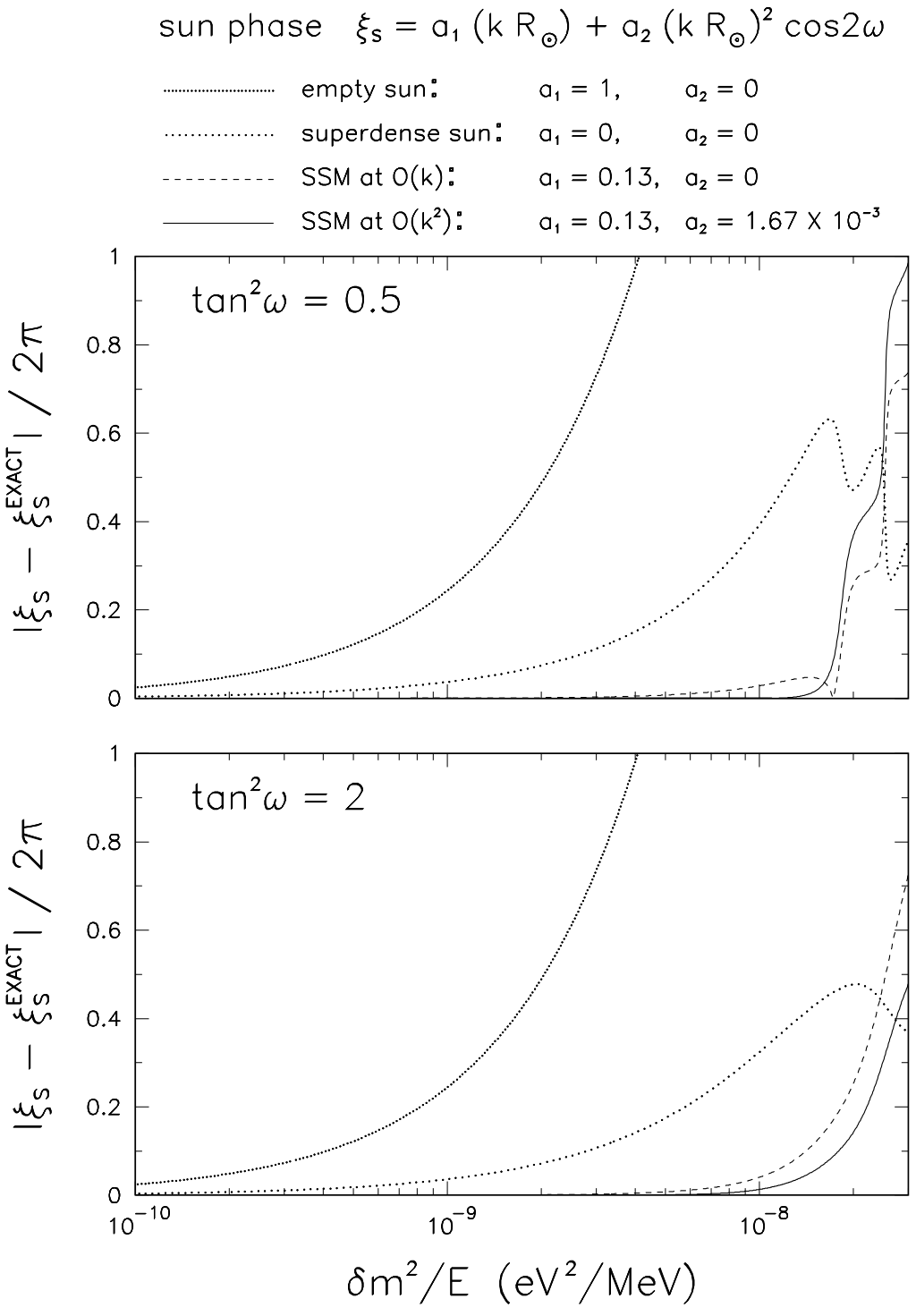

FIG. 10. The absolute error induced by approximate calculations of the solar phase ξ_s, as compared with the exact numerical calculations, in units of 2π. See the text for details.

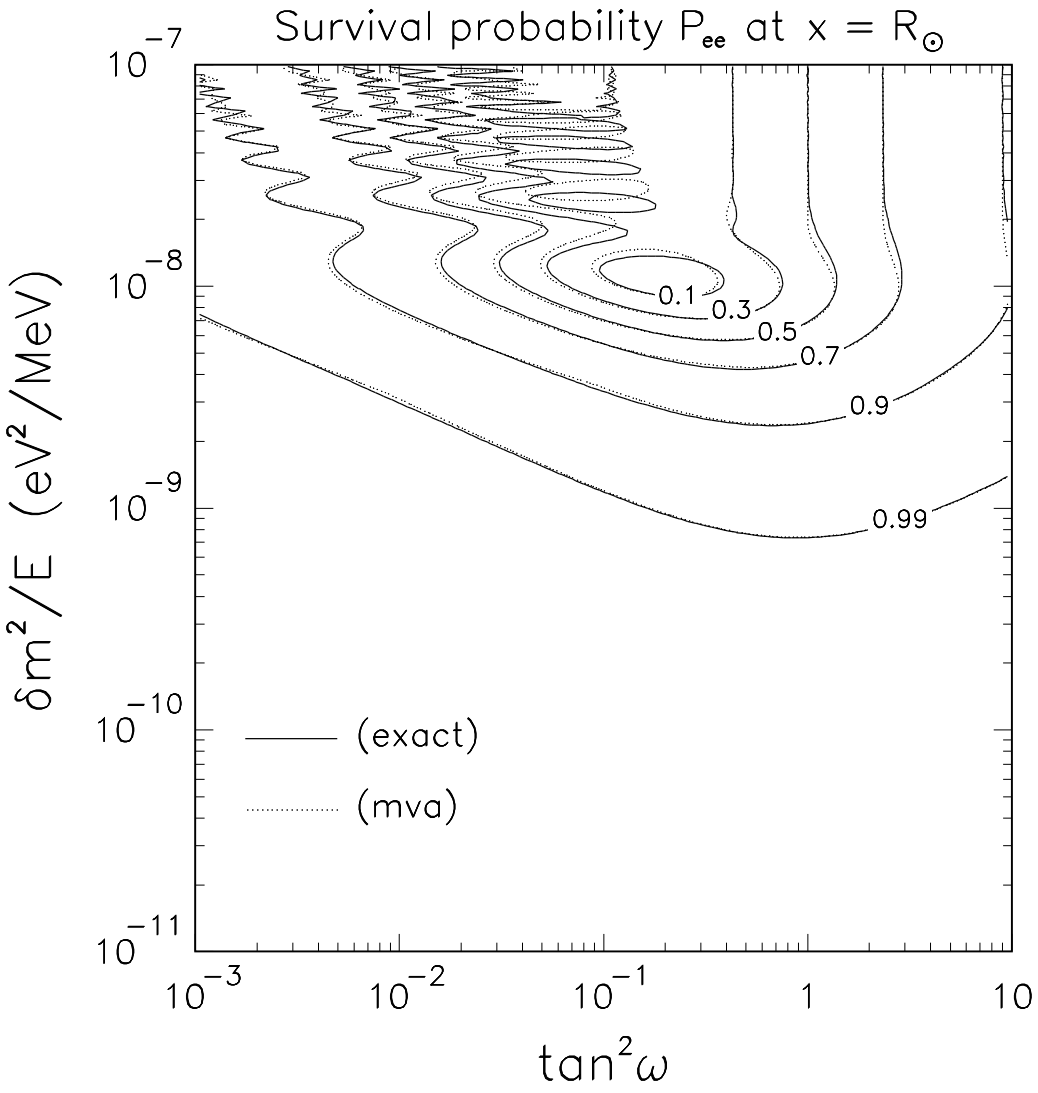

FIG. 11. Application of our final analytical recipe for P_c and ξ_s to the calculation of $P_{ee}(R_\odot)$ at the exit from the Sun (dotted lines), as compared with the corresponding exact numerical results (solid lines).